(12) INTERNATIONAL APPLICATION PUBLISHED UNDER THE PATENT COOPERATION TREATY (PCT)

(19) World Intellectual Property Organization
International Bureau

(43) International Publication Date
19 December 2024 (19.12.2024)

WIPO | PCT

(10) International Publication Number
WO 2024/256220 A1

(51) International Patent Classification:
G06F 7/544 (2006.01) *G06N 10/00* (2022.01) *G06E 3/00* (2006.01)

(21) International Application Number: PCT/EP2024/065333

(22) International Filing Date: 04 June 2024 (04.06.2024)

(25) Filing Language: English

(26) Publication Language: English

(30) Priority Data:
102023000012279 15 June 2023 (15.06.2023) IT

(71) Applicants: **UNIVERSITA' DEGLI STUDI DI ROMA "LA SAPIENZA"** [IT/IT]; PIAZZALE ALDO MORO 5, I-00185 Roma (RM) (IT). **INTERNATIONAL IBERIAN NANOTECHNOLOGY LABORATORY** [PT/PT]; AVENIDA MESTRE JOSÉ VEIGA n/a, 4715-330 Braga (PT). **CONSIGLIO NAZIONALE DELLE RICERCHE** [IT/IT]; PIAZZALE ALDO MORO 7, I-00185 Roma (RM) (IT).

(72) Inventors: **FAGUNDES GALVÃO, Ernesto**; c/o INTERNATIONAL IBERIAN NANOTECHNOLOGY LABORATORY, AVENIDA MESTRE JOSÉ VEIGA n/a, 4715-330 Braga (PT). **SCIARRINO, Fabio**; c/o UNIVERSITA' DEGLI STUDI DI ROMA "LA SAPIENZA", PIAZZALE ALDO MORO 5, I-00185 Roma (RM) (IT). **CARVACHO VERA, Gonzalo Alfredo**; c/o UNIVERSITA' DEGLI STUDI DI ROMA "LA SAPIENZA", PIAZZALE ALDO MORO 5, I-00185 Roma (RM) (IT). **HOCH, Francesco**; c/o UNIVERSITA' DEGLI STUDI DI ROMA "LA SAPIENZA", PIAZZALE ALDO MORO 5, I-00185 Roma (RM) (IT). **SPAGNOLO, Nicolò**; c/o UNIVERSITA' DEGLI STUDI DI ROMA "LA SAPIENZA", PIAZZALE ALDO MORO 5, I-00185 Roma (RM) (IT). **OSELLAME, Roberto**; c/o CONSIGLIO NAZIONALE DELLE RICERCHE, PIAZZALE ALDO MORO 7, I-00185 Roma (RM) (IT). **GIORDANI, Taira**; c/o UNIVERSITA' DEGLI STUDI DI ROMA "LA SAPIENZA", PIAZZALE ALDO MORO 5, I-00185 Roma (RM) (IT). **CASTELLO, Luca**; c/o UNIVERSITA' DEGLI STUDI DI ROMA "LA SAPIENZA", PIAZZALE ALDO MORO 5, I-00185 Roma (RM) (IT).

(74) Agent: **PERRONACE, Andrea** et al.; c/o Jacobacci & Partners S.p.A., via Tomacelli, 146, I-00186 Roma (IT).

(81) Designated States *(unless otherwise indicated, for every kind of national protection available)*: AE, AG, AL, AM, AO, AT, AU, AZ, BA, BB, BG, BH, BN, BR, BW, BY, BZ, CA, CH, CL, CN, CO, CR, CU, CV, CZ, DE, DJ, DK, DM, DO, DZ, EC, EE, EG, ES, FI, GB, GD, GE, GH, GM, GT, HN, HR, HU, ID, IL, IN, IQ, IR, IS, IT, JM, JO, JP, KE, KG, KH, KN, KP, KR, KW, KZ, LA, LC, LK, LR, LS, LU, LY, MA, MD, MG, MK, MN, MU, MW, MX, MY, MZ, NA, NG, NI, NO, NZ, OM, PA, PE, PG, PH, PL, PT, QA, RO,

(54) **Title:** QUANTUM BERNOULLI FACTORY PHOTONIC CIRCUIT INDEPENDENT OF INPUT STATE BIAS

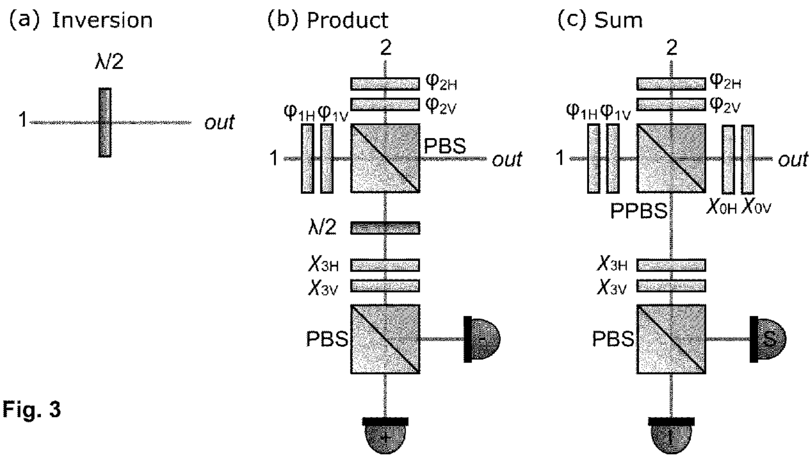

Fig. 3

(57) **Abstract:** The present invention concerns a scheme that allows to create a Quantum-to-Quantum Bernoulli Factory, wherein random bits and qubits can be generated given input qubits, using a quantum photonic system that can take advantage of the different information coding approaches using states of single photons According to the invention, inversion, multiplication and sum operations can be realized with photon qubits and can be concatenated without generating noise.

WO 2024/256220 A1

[Continued on next page]

RS, RU, RW, SA, SC, SD, SE, SG, SK, SL, ST, SV, SY, TH, TJ, TM, TN, TR, TT, TZ, UA, UG, US, UZ, VC, VN, WS, ZA, ZM, ZW.

(84) Designated States *(unless otherwise indicated, for every kind of regional protection available)*: ARIPO (BW, CV, GH, GM, KE, LR, LS, MW, MZ, NA, RW, SC, SD, SL, ST, SZ, TZ, UG, ZM, ZW), Eurasian (AM, AZ, BY, KG, KZ, RU, TJ, TM), European (AL, AT, BE, BG, CH, CY, CZ, DE, DK, EE, ES, FI, FR, GB, GR, HR, HU, IE, IS, IT, LT, LU, LV, MC, ME, MK, MT, NL, NO, PL, PT, RO, RS, SE, SI, SK, SM, TR), OAPI (BF, BJ, CF, CG, CI, CM, GA, GN, GQ, GW, KM, ML, MR, NE, SN, TD, TG).

Published:

— *with international search report (Art. 21(3))*

— *in black and white; the international application as filed contained color or greyscale and is available for download from PATENTSCOPE*

Quantum Bernoulli Factory photonic circuit independent of input state bias

------

Applicants: Università degli Studi di Roma "La Sapienza" (70%) International Iberian Nanotechnology Laboratory (20%), Consiglio Nazionale delle Ricerche (10%)

Inventors: Ernesto Fagundes Galvão (INL, 20%), Fabio Sciarrino (Sapienza Università di Roma, 15%), Gonzalo Alfredo Carvacho Vera (Sapienza Università di Roma, 15%), Francesco Hoch (Sapienza Università di Roma, 15%), Nicolò Spagnolo (Sapienza Università di Roma, 14%), Roberto Osellame (CNR-IFN, 10%), Taira Giordani (Sapienza Università di Roma, 6%), Luca Castello (Sapienza Università di Roma, 5%)

The present invention concerns a Quantum Bernoulli Factory photonic circuit independent of input state bias.

Background Art

The field of Quantum Information exploits the peculiarity of quantum effects as a new computational resource for faster computation, to enable unbreakable cryptographic protocols and to increase communication efficiency in distributed computational problems. Randomness plays an essential role in several research fields and numerous applications of information technology. Quantum mechanics gives access to genuine randomness based on the intrinsic random behavior of its measurement process. This peculiar property of quantum theory leads to numerous advantages in information manipulation, communication and processing, which have been exploited in various quantum communication protocols and quantum computing algorithms. The generation and manipulation of quantum randomness has been studied in depth and widely implemented using different platforms, single photon properties and protocols.

Random number handling is fundamental for statistical methods and computation. An interesting paradigm in this area are the so-called **Bernoulli factories**. These are randomness processing protocols that take as inputs random variables such as a coin with some bias, and change the bias in a well-defined way, which is independent of the bias. As a simple example, a first protocol is attributed to Von Neumann. Such a protocol that takes as input two coins of bias p and provides as output a coin with bias p'=1/2. This represents a useful task in processing randomness from practical random number generators and it is a first instance of a Bernoulli Factory. First introduced by Keane and O'Brien [1], the Bernoulli Factory concept addresses the problem of how to construct a variable distributed according to a Bernoulli distribution (an unbalanced coin), having access to another Bernoulli variable of unknown bias, aiming to obtain a certain functional relationship between the input and output distributions.

With reference to Fig. 1, the concept of a **Classical-to-Classical Bernoulli Factory (CCBF)** was then introduced, where both input and output are classical variables, finding applications in a wide range of fields ranging from Monte-Carlo simulation of Markov chains [2] to economy [3]. In Ref. [1] the space of simulable functions has been characterized, however a general method to be able to build them efficiently has not been found yet.

More concretely, Bernoulli Factories have proved useful for improving the performance of the Markov Chain Monte Carlo (MCMC) method, used to sample from complex probability distributions, as required for some simulation methods. In some situations, Bernoulli Factories can be used to avoid the need for a long burn-in period required in the process MCMC to sample from a good approximation of the target distribution [4]. In this context, Bernoulli factories have been used in simulations, for example of ocean currents [5], as well as in economics and game theory [6, 3]. These applications of classical Bernoulli Factories allow us to predict advantages in its consistent use in a quantum computational environment, possibly by combining their properties with other quantum algorithmic primitives, known in the field as amplitude and phase estimation.

In recent years the problem was extended to the quantum domain by analyzing the possibility of replacing the input and/or output Bernoulli variables with quantum analogues. In Ref. [7, 8], Dale et al. proposed the first quantum version of the Bernoulli Factory considering a quantum input and a classical output: a Quantum-to-Classical Bernoulli Factory (QCBF). The QCBF manipulates a Bernoulli variable encoded by a quantum coin (or quoin) as an input parameter. A quoin is a qubit in a pure state which, when measured in the computational basis, returns a classical Bernoulli variable. As the first connection between fully classical CCBF and the **Quantum-to-Classical Bernoulli Factory (QCBF)** it is observed that all of the functions that can be implemented by a CCBF can also be implemented by a QCBF extension. Indeed, it is sufficient to measure the quoin in the computational basis to recover a Bernoulli variable with the same bias parameter. In reference [7] the space of functions simulable by a QCBF has been characterized, showing that it is strictly larger than the purely classical case (CCBF).

Furthermore, it has also been demonstrated that a change of basis is the only quantum operation necessary to implement the whole set of simulable functions. There is evidence showing that in the quantum case there is an advantage in terms of input coin extractions [9,10] even for functions that can be classically simulated. A more complex quantum extension of the Bernoulli Factory was later proposed by Jiang et al. [11] where both input and output are quoins: A **Quantum-to-Quantum Bernoulli Factory (QQBF)**. Thus, the output can be used as an input for other quantum algorithms. In Ref. [8], the set of simulable functions of a QQBF has been fully characterized and a procedure to construct them in the circuit paradigm of quantum computing has been defined. It is important to note that for any version of the Bernoulli factory its implementation must be the same regardless of input state bias, i.e. the protocol must not use any information on the input state. No previous attempt to implement a QQBF [12,13] has been able to guarantee this condition when one wishes to combine individual operations (see Table 1). In particular, Ref. [12] uses entangled photons as primary resource, which is however impossible to be employed in a subsequent step due to the performed measurement. In Ref. [13], the two input qubits are codified in different degrees of freedom of the same photon, and hence performing concatenation of multiple requires knowledge on the output state after the first step, which is forbidden by the protocol.

	Bernoulli Factory model	**Modularity of the scheme**	**Concaten. of operations**	**Coding of a qubit on a single photon**	**Information coding**	**Linear optics**
Ref. [13]	QQBF	X			Polarization and dual-rail	X
Ref. [12]	QQBF	X			polarization	X
Ref. [9]	QCBF				Spins, super-conductors	
Ref. [10]	QCBF			X	polarization	X

Moreover, today's implementations of QQBF do not allow to carry out all of the theoretically admissible transformations in a state-independent way, one of the main advantages of the protocol.

These limitations notwithstanding, the Quantum Bernoulli Factory turns out to be a general answer to the problem of generating new random variables both classical, like a random bit, and quantum, i.e. qubits, two-level quantum systems, quantum equivalents of bits. The potential advantages of the Quantum Bernoulli Factory are therefore wide-ranging and concern:

1. Constructible functions for classical random variables – By constructible functions we mean the transformations that operate on random variables with an unknown distribution to generate new ones. It has been shown that the class of functions constructible by a Quantum Bernoulli Factory is strictly larger than the functions constructible by the classical Bernoulli Factory.

2. Computational advantage – For the same function, the quantum version requires on average a smaller number of extractions. This implies that the use of a quantum system in the implementation of a Bernoulli Factory reduces the consumption of resources if this is compared with its classical equivalent.

3. Exact method – The Quantum Bernoulli Factory applies the required transformation exactly; its application does not need to introduce computational or approximation errors. This contrasts with classical Bernoulli Factories, where approximation methods are sometimes unavoidable.

The applications of this protocol also concern various areas of computation and communication in both the classical and quantum fields. In particular, the Quantum Bernoulli Factory offers benefits in the following scenarios:

1. Sampling algorithm subroutines. These algorithms aiming to sample from an unknown distribution, the most famous examples being the Markov Chain Monte Carlo methods, can benefit from the sampling properties of the Bernoulli Factory.

2. Quantum algorithm subroutines – Given the quantum nature of the method in both input and output this approach can be used as a basis function for more complex quantum programs.

3. Cryptography and ciphering - The distinctive property of the Quantum Bernoulli Factory is that it does not require knowledge of the probability distribution that governs the random variable of entrance. This makes it particularly useful in encryption protocols where it is generally necessary to process encrypted message strings for which it is not possible to know the probability distribution that determines their encryption, both in a quantum and traditional context.

4. Scenarios with multiple customers. The concept of the QQBF can be extended in the more general scenario of multiple users, i.e. the condition in which the factory takes as input several quoins. This formulation finds further application in quantum computing, more specifically in the framework of blind quantum computing [14].

A need is therefore felt to devise a Quantum-to-Quantum Bernoulli Factory that improves the existing versions and in particular guarantees that its implementation be the same regardless of input state bias, i.e. the protocol does not use any information on the input state, in order to combine individual operations.

Moreover, the development of the quantum technology market is strongly moving towards a "cloud computing" style approach, which must use NISQ (Noisy Intermediate-Scale Quantum) technology currently available in quantum computing. However, the manipulation of quantum states via current NISQ platforms is not suitable for a distributed approach, therefore a need is felt to have a Quantum Bernoulli Factory which can be used in distributed environments.

Object and subject matter of the invention

The object of the present invention is to provide a Quantum-to-Quantum Bernoulli Factory method that solve the problems and overcome the disadvantages of the prior art.

The subject-matter of the present invention is a Quantum-to-Quantum Bernoulli Factory method according to the attached claims.

Detailed description of embodiments of the invention

List of figures

The invention will now be described for illustrative but non-limiting purposes, with particular reference to the drawings of the attached figures, wherein:

- Fig. 1 shows different types of Bernoulli Factories according to the prior art: (a) Classical-to-Classical Bernoulli Factory (CCBF) where a sequence of classical bits with unknown bias p are processed to produce a new coin with bias f(p); (b) Quantum-to-Classical Bernoulli Factory (QCBF) in which a quantum coin (Quoin) encodes the input bias in quantum amplitudes, with the goal of generating classical coins with a different bias; (c) Quantum-to-Quantum Bernoulli Factory (QQBF) where both the input and output are quantum states;
- Fig. 2 shows the block scheme of the Modular Optical Quantum Bernoulli Factory (MOQBEF) with reference to the creation and annihilation operators for the electromagnetic field modes, and to the corresponding logical encoding for the qubits in the computational basis ($|0_L\rangle$,$|1_L\rangle$). The annihilation and creation operators refer to generic modes of the electromagnetic fields, and can correspond to any possible choice of degree of freedom for qubit encoding, thus independent from the specific implementation; (a) Inversion operation is performed by applying a suitable transformation $U_{inversion}$ to the input qubit; (b) Product operation is obtained by

applying a suitable transformation $U_{product}$ to the four input modes, which correspond to two input qubits when one photon is present in each mode pair, and conditioned to the detection of one photon in output $+$; (c) Sum operation is obtained by applying a suitable transformation U_{sum} to the four input modes, which corresponds to two input qubits when one photon is present in each mode pair, and conditioned to the detection of one photon in output S;

– Fig. 3 shows building blocks for a polarization implementation according to the present disclosure. The inputs of the interferometers are labeled by numbers 1 and 2, while the output is labeled as *out*; (a) Inversion operation is performed by propagation of the input qubit through a half-wave plate with optical axis oriented at an angle of π/4 to the horizontal axis. (b) Product operation is performed by applying a set of phase shifts on the input photons, different for each polarization state, by injecting them in the two input ports of a polarizing beam splitter, and post-selecting the events for which one photon exits from each port. One of the outputs propagates through a half-wave plate with optical axis rotated by π/8 with respect to the horizontal one, followed by two phase shifts different for each polarization state, and a measurement in the computational basis. Depending on the obtained outcome, the other photon is in the product or in the anti-product state; (c) The sum operation is performed by making two photons interfere in a partially-polarizing beam splitter after application of a set of two phase shifts on the input photons, different for each polarization state, and post-selecting the events where the two photons exit from different ports. A polarizing beam splitter is applied to separate the photons and to measure one of them after a set of phase shifts different for each polarization state are applied on each output photon. Depending on the outcome of the measurement in the computational basis, the other photon will be found in the “sum” or “harmonic mean” state;

- Fig. 4 shows an implementation of the conversion between time encoding and polarization encoding according to the disclosure. This step allows the same schemes used for the polarization to be used also for time encoding. Legend: EOM electro-optical modulator, PBS: polarizing beam-splitter (polarizing semi-reflective mirror), DL: delay line;
- Fig. 5 shows building blocks for MOQBEF based on path encoding. The input ports of the interferometers are labelled 1 and 2, with outputs labelled *out*: (a) Inversion is performed deterministically by swapping the dual-rail modes; (b) The product is performed by applying a set of phase shifts $(\varphi_1, \varphi_2, \varphi_3, \varphi_4)$ on the input components of the qubits, by sending the component 1_L of dual-rail qubit 1 and component 0_L of dual-rail qubit 2 into a balanced beam-splitter, by applying two phase shifts (χ_2, χ_3) on the output modes of the beam-splitter, and post-selecting events with one of the two photons in output ports - or + in the figure. The state prepared by this measured event is encoded in an output dual-rail qubit labelled *out*; (c) The sum is implemented by swapping the input mode component 1_L of dual-rail qubit 1 and component 0_L of dual-rail qubit 2, by applying a set of phase shifts $(\varphi_1, \varphi_2, \varphi_3, \varphi_4)$ on the input components of the qubits, by directing the modes in two beam-splitters, and by applying a second set of phase shifts $(\chi_1, \chi_2, \chi_3, \chi_4)$ on the output modes. Here, also, the operation is successful when a photon is detected by the detector labelled “S”;
- Fig. 6 shows an implementation of the conversion between orbital angular momentum and path according to the disclosure. This step allows the same schemes used for the path to be used also for orbital

angular momentum encoding. Legend: OAM orbital angular momentum;

- Fig. 7 shows an implementation of the conversion between frequency-bin and path according to the disclosure. This step allows the same schemes used for the path to be used also for frequency encoding. Legend: WD wavelength demultiplexing, QFP quantum frequency processor;
- Fig. 8 shows a prototype of the MOQBF acting on an input of 3 dual-rail qubits, according to an embodiment of the disclosure. Thermo-optic effect devices can control the reflectivities of the beam-splitters in panel a, as well as the phase shifters represented by rectangles in the schematic. The beam-splitters with tunable beam-splitting ratios can be implemented via a Mach-Zehnder interferometer featuring two 50/50 beam-splitters and a phase shifter in between (inset b);
- Fig. 9 shows a configuration for the implementation of the building blocks of the MOQBEF in a 6-mode reprogrammable interferometer, according to an embodiment of the disclosure. (a) Product operation. Here, we use the ports 3-6 for both input and output. (b) Addition/sum operation. Here we use the ports 1-4 at the input, and 1-2,4-5 at the output;
- Fig. 10 shows concatenations of two operations in the MOQBEF encoded in a 6-mode reprogrammable interferometer, according to an embodiment of the disclosure. (a) Addition followed by product operation. The output qubit $|z_4\rangle = |(z_1 + z_2)z_3\rangle$is found at ports 4-5, when the other two photons are detected in the output mode pairs (1,2), (3,6). (b) Addition/sum operation. The output qubit $|z_1 z_2 + z_3\rangle$ is encoded in the modes 3-4 when the other two photons are detected in the mode pairs (1,5), (2,6); and
- Fig. 11 shows an example of a MOQBF acting on 5 dual-rail path encoded qubits, according to an embodiment of the disclosure. This

photonic circuit implements the following function: $|z\rangle = |z_1 z_2 z_3 + z_4 z_5\rangle$.

It is specified here that elements of different embodiments can be combined together to provide further embodiments without limits respecting the technical concept of the invention, as the average person skilled in the art understands without problems from what has been described.

The present description also refers to the prior art for its implementation, with regards to the detailed characteristics not described, such as for example minor elements usually used in the prior art in solutions of the same type.

When introducing an element, it is always understood that it can be "at least one" or "one or more".

When a list of elements or characteristics is listed in this description it is meant that the invention according to the invention "comprises" or alternatively "is composed of" such elements.

When listing features within the same sentence or bulleted list, one or more of the individual features may be included in the invention without connection to the other features in the list.

Two or more of the parts (elements, devices, systems) described above can be freely associated and considered as a kit of parts according to the invention.

Embodiments

Introduction

In this disclosure we introduce a scheme that allows to create on the one hand a more general Quantum Bernoulli Factory, i.e. one in which random bits or qubits can be generated given an input qubit, and on the other hand to reproduce all the above-listed properties and advantages of the protocol. The disclosure provides for an implementation using a

quantum photonic system that can take advantage of the different information coding approaches using states of single photons. The validity of the proposed scheme has already been experimentally verified by the Inventors in an integrated and fully reconfigurable photonics platform.

Let us therefore examine in detail the various characteristics of the disclosure. As anticipated, we introduce a photonic **modular approach** to realize an arbitrary Quantum-to-Quantum Bernoulli Factory. Hereafter we will refer to the disclosure device as the Modular Optical Quantum Bernoulli Factory (MOQBEF).

In the context of emerging quantum processors, the MOQBEF fits fully into the framework of NISQ (Noisy Intermediate-Scale Quantum) technologies. In the next decade or so, full quantum error correction is not expected to be achieved in any technological platform, making it essential to map capabilities and limitations of current noisy quantum technologies. The scheme proposed below follows this approach, and it is therefore possible to implement it starting from the current state of the art with photonic platforms. However, the only limitation of the proposed photonic coding procedure is its probabilistic nature. That is, the known function to be applied to the random variables is implemented with a given probability of success. However, it is observed that the manipulation of quantum states via other NISQ technologies platforms is according to the current state of the art not suitable for a distributed approach (for example, through superconducting devices, trapped ions, etc.). Currently, the development of the quantum technology market is strongly moving towards a "cloud computing" style approach, given the current complexity and costs of the various platforms. In order to coherently distribute the resources manipulated through other NISQ platforms to more customers, it would in any case be necessary to transfer the information to photonic qubits, introducing significant losses and additional sources of noise, being overall clearly disadvantageous compared to a scheme implemented entirely by a photonic approach like that of the MOQBEF. Furthermore, current single photon manipulation technologies (bulk optics, integrated photonics) do not require complex cryogenic apparatus and can be implemented in miniaturized cryogenic units (also exploiting the strong technological maturity of photonic technologies for communication).

Basic features

The space of functions that can be constructed using a Quantum Bernoulli Factory has a mathematical field structure [11]; therefore to reach an arbitrary Quantum-to-Quantum Bernoulli Factory it is necessary to demonstrate:

A. The realization of 3 building blocks corresponding to the fundamental operations of the field (**addition/sum, product and inverse operations**).

B. The possibility of combining the operations of the previous point in order to realize an arbitrary function. For this purpose, the approach proposed in the present disclosure exploits single photon states to encode the input and output qubits. In particular, we will refer to five different encodings:

1. **polarization:** where the two basic logical quantum states are associated with two orthogonal polarizations of the electromagnetic field, usually chosen as vertical and horizontal;
2. **time (also called "time-bin"):** in this case the two basic quantum states $|0_L\rangle$ and $|1_L\rangle$ are associated with two completely distinct time intervals;
3. **path (also called “dual rail”):** where a single photon present in one of two propagation paths of light encodes logical states $|0_L\rangle$ or $|1_L\rangle$.
4. **orbital angular momentum (OAM):** the logical quantum levels are two eigenstates of the orbital angular momentum operator of the electromagnetic field.

5. **frequency (also called "frequency-bin):** here the two quantum logical levels $|0_L\rangle$ and $|1_L\rangle$ are two distinct optical frequencies.

In each of the three encodings and implementations of the protocol, the MOQBEF according to the disclosure scheme provides different solutions to the problems and limitations of the prior art. In fact, it first solves the problem of modularity, i.e. the possibility of implementing both individually and in combination the 3 fundamental blocks that implement the single field operations. This makes it possible to implement the entire spectrum of functions that can be constructed from a Quantum-to-Quantum Bernoulli factory. Finally, these functions are applied to the state's random input without the requirement to know the original probability distribution. The latter property is essential for a genuine creation of a Quantum-to-Quantum Bernoulli Factory. In addition, the MOQBEF exploits a photonic platform that has been greatly developed in recent years, and offers technological advantages provided by encoding quantum systems in single photon states. In fact, they can be processed using linear optical elements, such as waveplates and semi-reflecting mirrors for bulk optics setup, or waveguides with directional couplers and controlled phase delays for integrated photonics. The photonic states generated by the MOQBEF will also be able to be distributed among multiple parties and customers, using traditional fiber optic signal transmission channels. Other possible choices of the encodings include orbital angular momentum, associated to the spatial and phase field distribution, or frequency-based encoding. Orbital angular momentum can be manipulated via several devices, including vortex plates, q-plates and spatial-light modulators. Frequency encoding is based on assigning the qubit logical values $|0\rangle_L$ and $|1_L\rangle$ to different distinct frequencies of the field. This degree of freedom can be manipulated by means of pulse shaping systems, and electro-optical modulators.

The technical characteristics of the three possible photonic encodings of the MOQBEF are analyzed below. First of all, it is necessary to formally define the operations of the MOQBEF. The input variable of a MOQBEF is a quantum state of the type $\frac{z|0_L\rangle+|1_L\rangle}{\sqrt{1+|z|^2}}$ where z can be either a real or a complex number. Therefore, the elementary operations are:

- Inversion: $f(z) = 1/z$;
- Addition/sum: $f(z_1, z_2) = z_1 + z_2$;
- Product: $f(z_1, z_2) = z_1 z_2$

In the following sections we will describe the possible encoding and processing of such operations in the degrees of freedom of single-photon states. We will show the details of each field operation and, in particular, the resource cost in terms of quoins. For example, the sum and the product necessarily require the measurement of one quoin, while the inversion does not.

Block scheme

The block scheme of the MOQBEF is shown in Figure 2 in an implementation-independent way. The inversion operation (Figure 2(a)) is a single-photon transformation, and is obtained by applying a suitable unitary transformation, that we label as $U_{inversion}$, on the input modes. Conversely, the product and sum operations require two input photons, and are obtained (Figure 2(b-c)) after application of suitable unitary transformations, that we label as $U_{product}$ and U_{sum} respectively, and conditioned to the detection of one photon in one specific output (labeled as $+$ for the product in panel b, and as S for the sum in panel c). For an optimal implementation of the MOQBEF in terms of number of modes, we require that each block is implemented via a transformation acting on the exact number of modes corresponding to the number of qubits (2 modes for each qubit). This corresponds to the requirement that the blocks perform linear unitary operations.

The functions realized by the various blocks are as follows.

The transformation $U_{inversion}$ to be applied on the input modes can be derived by considering the input state $|z\rangle$ and a 2×2 unitary evolution U, with matrix elements u_{ij}, acting linearly on the creation and annihilation mode operators according to $b_j^\dagger = \sum_k u_{jk} a_k^\dagger$, where $b_j^\dagger$ are the mode operators after the action of the transformation, and $a_k^\dagger$ are the mode operators before the transformation. The necessary transformation to obtain the inversion requires to exchange the input modes, thus corresponding to a logical exchange of the basis states of the qubit ($|0_L\rangle, |1_L\rangle$), and thus has the following form:

$$U_{inversion} = \begin{pmatrix} 0 & 1 \\ 1 & 0 \end{pmatrix}$$

The transformation $U_{product}$ to be applied on the input modes can be derived by considering two input states $|z_1\rangle$ and $|z_2\rangle$, according to Figure 2b, and a 4×4 unitary evolution U, with matrix elements u_{ij}, acting linearly on the creation and annihilation mode operators according to $b_j^\dagger = \sum_k u_{jk} a_k^\dagger$, where $b_j^\dagger$ are the mode operators after the action of the transformation, and $a_k^\dagger$ are the mode operators before the transformation. We then write the input states as $|z_1\rangle = \frac{z_1 a_1^\dagger + a_2^\dagger}{\sqrt{1+|z_1|^2}} |\emptyset\rangle$ and $|z_2\rangle = \frac{z_2 a_3^\dagger + a_4^\dagger}{\sqrt{1+|z_2|^2}} |\emptyset\rangle$ at the input of the scheme of Figure 2b, being $|\emptyset\rangle$ the vacuum state. After application of the transformation U, we post-select on one photon detected on mode 3, while the other photon is present on mode pair 1-4 (corresponding to logical qubits $|0_L\rangle_{out}$ and $|1_L\rangle_{out}$). We find that the resulting state (up to a normalization factor) after the operation reads:

$$
\begin{aligned}
|\psi_O\rangle = \{&[(u_{12}u_{34} + u_{32}u_{14})b_1^\dagger + (u_{42}u_{34} + u_{32}u_{44})b_4^\dagger] \\
&+ z_1[(u_{11}u_{34} + u_{31}u_{14})b_1^\dagger + (u_{41}u_{34} + u_{31}u_{44})b_4^\dagger] \\
&+ z_2[(u_{13}u_{32} + u_{33}u_{12})b_1^\dagger + (u_{43}u_{32} + u_{33}u_{42})b_4^\dagger] \\
&+ z_1 z_2[(u_{11}u_{33} + u_{31}u_{13})b_1^\dagger + (u_{41}u_{33} + u_{31}u_{43})b_4^\dagger]\}|\emptyset\rangle
\end{aligned}
$$

To obtain the output product state $|z_1 z_2\rangle$, we then impose that state $|\psi_O\rangle$ is equal to $|z_1 z_2\rangle = (z_1 z_2 b_1^\dagger + b_4^\dagger)|\emptyset\rangle$. This requirement corresponds to adding the following conditions on the matrix elements of U:

$$
\begin{gathered}
u_{12}u_{34} + u_{32}u_{14} = 0 \\
u_{11}u_{34} + u_{31}u_{14} = 0 \\
u_{41}u_{34} + u_{31}u_{44} = 0 \\
u_{13}u_{32} + u_{33}u_{12} = 0 \\
u_{43}u_{32} + u_{33}u_{42} = 0 \\
u_{41}u_{33} + u_{31}u_{43} = 0 \\
u_{42}u_{34} + u_{32}u_{44} = u_{11}u_{33} + u_{31}u_{13} \neq 0
\end{gathered}
$$

By starting to insert these conditions on the matrix elements u_{ij}, we first start from the condition $u_{12}u_{34} + u_{32}u_{14} = 0$. By multiplying this expression by u_{31} and subsequently by u_{33}, and using the last condition above, we first find that: $u_{32} = 0 \vee u_{34} = 0$. We consider the case $u_{34} = 0$ (similar procedure and analogous result is obtained for $u_{32} = 0$). We first obtain that the unitary matrix has to be reduced to:

$$
U = \begin{pmatrix} u_{11} & u_{12} & u_{13} & 0 \\ u_{21} & u_{22} & u_{23} & u_{24} \\ 0 & u_{32} & u_{33} & 0 \\ 0 & u_{42} & u_{43} & u_{44} \end{pmatrix}
$$

Using the orthonormality condition between the first and last columns, we find that the matrix can be reduced to:

$$
U = \begin{pmatrix} e^{i\lambda} & 0 & 0 & 0 \\ 0 & u_{22} & u_{23} & u_{24} \\ 0 & u_{32} & u_{33} & 0 \\ 0 & u_{42} & u_{43} & u_{44} \end{pmatrix}
$$

where λ is an arbitrary phase parameter between 0 and 2π. We now need to analyse the 3×3 unitary submatrix composed by rows 2,3,4 and columns 2,3,4, that we label as $\widetilde{U}$. We now exploit the decomposition of Ref. [15] for 3×3 unitary submatrix, which permits to express the remaining matrix elements as:

$$u_{22} = e^{i\phi_6}\left(-\sin\theta_1 \cos\theta_2 \sin\theta_3 \, e^{i(\phi_1-\phi_3+\phi_5)} - \sin\theta_2 \cos\theta_3 \, e^{-i(\phi_2+\phi_4)}\right)$$

$$u_{23} = e^{i\phi_6}\left(-\sin\theta_1 \cos\theta_2 \cos\theta_3 \, e^{i(\phi_1+\phi_2-\phi_3)} + \sin\theta_2 \sin\theta_3 \, e^{-i(\phi_4+\phi_5)}\right)$$

$$u_{24} = e^{i\phi_6}\left(\cos\theta_1 \cos\theta_2 \, e^{i\phi_1}\right)$$

$$u_{32} = e^{i\phi_6}\left(\cos\theta_1 \sin\theta_3 \, e^{i\phi_5}\right)$$

$$u_{33} = e^{i\phi_6}\left(\cos\theta_1 \cos\theta_3 \, e^{i\phi_2}\right)$$

$$u_{34} = e^{i\phi_6}\left(\sin\theta_1 \, e^{i\phi_3}\right)$$

$$u_{42} = e^{i\phi_6}\left(-\sin\theta_1 \sin\theta_2 \sin\theta_3 \, e^{i(-\phi_3+\phi_4+\phi_5)} + \cos\theta_2 \cos\theta_3 \, e^{-i(\phi_1+\phi_2)}\right)$$

$$u_{43} = e^{i\phi_6}\left(-\sin\theta_1 \sin\theta_2 \cos\theta_3 \, e^{i(\phi_2-\phi_3+\phi_4)} - \cos\theta_2 \sin\theta_3 \, e^{-i(\phi_1+\phi_5)}\right)$$

$$u_{44} = e^{i\phi_6}\left(\cos\theta_1 \sin\theta_2 \, e^{i\phi_4}\right)$$

with $0 \le \theta_1, \theta_2, \theta_3 \le \pi/2$ and $0 \le \phi_1, \ldots, \phi_6 \le 2\pi$. By setting element $u_{34} = 0$, this implies that $\theta_1 = 0$. The expression for the 3×3 unitary submatrix simplifies into:

$$\widetilde{U} = e^{i\phi_6} \begin{pmatrix} -\sin\theta_2 \cos\theta_3 e^{-i(\phi_2+\phi_4)} & \sin\theta_2 \sin\theta_3 e^{-i(\phi_4+\phi_5)} & \cos\theta_2 e^{i\phi_1} \\ \sin\theta_3 \, e^{i\phi_5} & \cos\theta_3 \, e^{i\phi_2} & 0 \\ \cos\theta_2 \cos\theta_3 e^{-i(\phi_1+\phi_2)} & -\cos\theta_2 \sin\theta_3 e^{-i(\phi_1+\phi_5)} & \sin\theta_2 e^{i\phi_4} \end{pmatrix}$$

Finally, by inserting the different constraint on the matrix elements reported above, and by relabelling the non-zero parameters, we obtain that the transformation $U_{product}$ has the following form:

$$U_{product} = \begin{pmatrix} e^{i(\phi_1+\phi_2-\phi_3)} & 0 & 0 & 0 \\ 0 & -\frac{e^{i\phi_2}}{\sqrt{2}} & \frac{e^{i\phi_3}}{\sqrt{2}} & 0 \\ 0 & \frac{e^{-i(\phi_3+\phi_4)}}{\sqrt{2}} & \frac{e^{-i(\phi_2+\phi_4)}}{\sqrt{2}} & 0 \\ 0 & 0 & 0 & e^{i\phi_1} \end{pmatrix}$$

where the parameters $(\phi_1, \phi_2, \phi_3, \phi_4)$ can take any value between 0 and 2π. When considering the case of 4-mode transformations that correspond to the optimal allocation of resources, the unitary transformation $U_{product}$ obtained above is unique. By "optimal allocation of resources" we mean the lowest number of modes. A use of more modes is still possible by expanding the space of modes by introducing modes which do not correspond to photons at the input of the function (therefore more inputs where no photons are provided).

The same procedure can be obtained for the sum operation. The transformation U_{sum} to be applied on the input modes can be derived by considering two input states $|z_1\rangle$ and $|z_2\rangle$, according to Figure 2c, and a 4×4 unitary evolution U, with matrix elements u_{ij}, acting linearly on the creation and annihilation mode operators according to $b_j^\dagger = \sum_k u_{jk} a_k^\dagger$, where $b_j^\dagger$ are the mode operators after the action of the transformation, and $a_k^\dagger$ are the mode operators before the transformation. We then write the input states as $|z_1\rangle = \frac{z_1 a_1^\dagger + a_2^\dagger}{\sqrt{1+|z_1|^2}} |\emptyset\rangle$ and $|z_2\rangle = \frac{z_2 a_3^\dagger + a_4^\dagger}{\sqrt{1+|z_2|^2}} |\emptyset\rangle$ at the input of the scheme of Figure 2c. After application of the transformation U, we post-select on one photon detected on mode 3, while the other photon is present on mode pair 1-4 (corresponding to logical qubits $|0_L\rangle_{out}$ and $|1_L\rangle_{out}$, wherein the subscript "out" can be omitted when already clear that this is a state at the output of the interferometer, as done in the claims). We find that the resulting state (up to a normalization factor) after the operation reads:

$$\begin{aligned}
|\psi_O\rangle = \{ & [(u_{12}u_{34} + u_{32}u_{14})b_1^\dagger + (u_{42}u_{34} + u_{32}u_{44})b_4^\dagger] \\
& + z_1[(u_{11}u_{34} + u_{31}u_{14})b_1^\dagger + (u_{41}u_{34} + u_{31}u_{44})b_4^\dagger] \\
& + z_2[(u_{13}u_{32} + u_{33}u_{12})b_1^\dagger + (u_{43}u_{32} + u_{33}u_{42})b_4^\dagger] \\
& + z_1 z_2[(u_{11}u_{33} + u_{31}u_{13})b_1^\dagger + (u_{41}u_{33} + u_{31}u_{43})b_4^\dagger]\}|\emptyset\rangle
\end{aligned}$$

To obtain the output sum state $|z_1 + z_2\rangle$, we then impose that state $|\psi_o\rangle$ is equal to $|z_1 + z_2\rangle = [(z_1 + z_2)b_1^\dagger + b_4^\dagger]|\emptyset\rangle$. This requirement corresponds to adding the following conditions on the matrix elements of U:

$$u_{12}u_{34} + u_{32}u_{14} = 0$$
$$u_{41}u_{34} + u_{31}u_{44} = 0$$
$$u_{43}u_{32} + u_{33}u_{42} = 0$$
$$u_{11}u_{33} + u_{31}u_{13} = 0$$
$$u_{41}u_{33} + u_{31}u_{43} = 0$$
$$u_{42}u_{34} + u_{32}u_{44} = u_{11}u_{34} + u_{31}u_{14} = u_{13}u_{32} + u_{33}u_{12} \neq 0$$

We first start by condition $u_{41}u_{33} + u_{31}u_{43} = 0$. By multiplying it by u_{32}, by using condition $u_{43}u_{32} + u_{33}u_{42} = 0$, and by multiplying the resulting expression by u_{34}, we finally obtain the condition $u_{33} = 0 \vee u_{31} = 0$. Regardless of which condition is chosen, the unitary matrix reduces to:

$$U = \begin{pmatrix} u_{11} & u_{12} & u_{13} & u_{14} \\ u_{21} & u_{22} & u_{23} & u_{24} \\ 0 & u_{32} & 0 & u_{34} \\ 0 & u_{42} & 0 & u_{44} \end{pmatrix}$$

where the matrix elements have to satisfy the following remaining conditions $u_{12}u_{34} + u_{32}u_{14} = 0, \quad u_{42}u_{34} + u_{32}u_{44} = u_{11}u_{34} = u_{13}u_{32}$. Using these conditions, and by inserting the orthonormality conditions between the matrix rows and columns, the matrix U can be further simplified as:

$$U = \begin{pmatrix} u_{11} & 0 & u_{13} & 0 \\ u_{21} & 0 & u_{23} & 0 \\ 0 & u_{32} & 0 & u_{34} \\ 0 & u_{42} & 0 & u_{44} \end{pmatrix}$$

Given the unitarity of the matrix, this transformation can be parameterized as:

$$U = \begin{pmatrix} \cos\theta_1 e^{i\phi_1} & 0 & \sin\theta_1 e^{i\phi_2} & 0 \\ \sin\theta_1 e^{-i(\phi_2+\phi_5)} & 0 & -\cos\theta_1 e^{-i(\phi_1+\phi_5)} & 0 \\ 0 & \cos\theta_2 e^{i\phi_3} & 0 & \sin\theta_2 e^{i\phi_4} \\ 0 & \sin\theta_2 e^{-i(\phi_4+\phi_6)} & 0 & -\cos\theta_2 e^{-i(\phi_3+\phi_6)} \end{pmatrix}$$

with $0 \leq \theta_1, \theta_2 \leq \pi/2$ and $0 \leq \phi_1, \ldots, \phi_6 \leq 2\pi$. By setting the constraints $u_{42}u_{34} + u_{32}u_{44} = u_{11}u_{34} = u_{13}u_{32}$, we finally obtain, after relabelling of the parameters, that transformation U_{sum} to be applied on the input modes has the following form:

$$U_{sum} = \begin{pmatrix} -\sqrt{\frac{5+\sqrt{5}}{10}}e^{i\phi_1} & 0 & \sqrt{\frac{5-\sqrt{5}}{10}}e^{i\phi_2} & 0 \\ \sqrt{\frac{5-\sqrt{5}}{10}}e^{-i(\phi_2+\phi_3)} & 0 & \sqrt{\frac{5+\sqrt{5}}{10}}e^{-i(\phi_1+\phi_3)} & 0 \\ 0 & -\sqrt{\frac{5+\sqrt{5}}{10}}e^{-i(\phi_2+\phi_4)} & i\sqrt{\frac{5+\sqrt{5}}{10}} & \sqrt{\frac{5-\sqrt{5}}{10}}e^{-i(\phi_1+\phi_4)} \\ 0 & \sqrt{\frac{5-\sqrt{5}}{10}}e^{i\phi_1} & 0 & \sqrt{\frac{5+\sqrt{5}}{10}}e^{i\phi_2} \end{pmatrix}$$

where the parameters $(\phi_1, \phi_2, \phi_3, \phi_4)$ can take any value between 0 and 2π. It can be shown that, when considering the case of 4-mode transformations that correspond to the optimal allocation of resources, the unitary transformation U_{sum} obtained above is unique.

Less efficient implementations can be obtained by allowing additional empty modes at the input, where no photons are injected, which have to be further discarded at the output. The transformation is then a unitary matrix U in the enlarged mode space, while it is described by a non-unitary matrix M in the qubit modes. As an example, with 2 additional empty modes, the sum can be implemented via the following matrix:

$$M_{sum} = \begin{pmatrix} \frac{i}{2} & 0 & \frac{i}{\sqrt{2}} & 0 \\ 0 & -\frac{i}{2} & 0 & \frac{i}{\sqrt{2}} \\ -\frac{1}{2} & 0 & \frac{1}{\sqrt{2}} & 0 \\ 0 & \frac{i}{2} & 0 & \frac{i}{\sqrt{2}} \end{pmatrix}$$

which leads to a less efficient implementation.

In the following we detail schemes for the implementations of these blocks in different encodings as anticipated above.

Polarization photonic operations

By exploiting the polarization degree of freedom, it is possible to construct the three building blocks previously mentioned in a compact and simple way. More specifically, in this encoding the two quantum levels correspond to two orthogonal polarization states as $|0_L\rangle = |H\rangle$, and $|1_L\rangle = |V\rangle$, where $|H\rangle$ and $|V\rangle$ stand respectively for horizontal and vertical linear polarization states. The generic input is then encoded as $|z\rangle = \frac{z|H\rangle+|V\rangle}{\sqrt{1+|z|^2}}$.

The building blocks for the polarization implementation of MOQBEF are depicted in Figure 3. The inputs of the interferometers are labeled by numbers 1 and 2, while the output is labeled as *out*. In operation block (a), the inversion operation is performed by propagation of the input qubit through a half-wave plate with optical axis oriented at an angle of π/4 to the horizontal axis. In operation block (b), the product operation is performed by applying phase shifts $(\varphi_{1H}, \varphi_{1V})$ on the two polarization states of photon 1, and phase shifts $(\varphi_{2H}, \varphi_{2V})$ on the two polarization states of photon 2. Then, the two photons are injected in the two input ports of a polarizing beam splitter (PBS), and post-selecting the events for which one photon exits from each port. One of the outputs propagates through a half-wave plate with optical axis rotated by π/8 with respect to the horizontal one, followed by two phase shifts (χ_{3H}, χ_{3V}) acting on the two polarization states, a PBS and photodetectors configured to measure the output in the computational basis. Depending on the obtained outcome, the other photon on output port *out* is in the product ($|z_1 z_2\rangle$) or in the anti-product state ($|-z_1 z_2\rangle$). In operation block (c), the addition operation is performed by applying phase shifts $(\varphi_{1H}, \varphi_{1V})$ on the two polarization states of photon 1, and phase shifts $(\varphi_{2H}, \varphi_{2V})$ on the two polarization states of photon 2. Then, the two photons interact in a partially-polarizing beam splitter (PPBS), that is, a beam-splitter with different reflectivities R_H and R_V for the two polarizations, and the output is post-selected on events where the two photons exit from different ports. After application of phase shifts (χ_{0H}, χ_{0V}) on the two polarization states of the photon present in output mode *out*, and phase shifts (χ_{3H}, χ_{3V}) on the two polarization states of the photon present in the other output port of the PPBS, a polarizing beam splitter is applied to measure the second one.. Depending on the outcome of the measurement, the photon on mode *out* will be found in the "sum" ($|z_1 + z_2\rangle$) or "harmonic mean" state ($\left|\frac{z_1 z_2}{z_1 + z_2}\right\rangle$).

The Inversion operation will thus be the operation that transforms the polarization state from $|H\rangle$ to $|V\rangle$ and vice versa, which indeed can be accomplished with a half wave delay plate. The realization of the remaining operations requires the interference between the polarization components of two single photons prepared in the states z_1 and z_2. In the interference process that occurs in partially-polarizing beam-splitters and polarizing beam splitters (see Figure 3), the indistinguishability of photons plays a fundamental role, which represents an exclusive and distinctive property of quantum systems. The probability of success of the operations of addition and product are conditioned on the presence of one of the two photons in the detectors marked by "+" and "-" in (b) and in "S" and "I" in (c).

To be more specific, the photon can be found in both photodetectors but this event will be discarded in the method according to the present disclosure. Conversely, none of the photon can be found in the photodetectors, and this event is discarded as well. The only events recognized as significant are those when a photon is found in either one or the other photodetector, and the other photon is found in the output port. This allows to have ideally zero noise in the device according to the disclosure. Some residual noise may come from the specific components used but is not due to the method. The zero-noise feature comes at the cost of waiting more time (statistically determined, see below) for the correct result to appear, or repeating the generation and measurement of the photons several times to increase the overall throughput.

The qubit resulting from the operation will be encoded in the polarization of the photon that leaves the device in the output port marked as *out* in Figure 3. This is because a specific polarization is set as 0-state and another as the 1-state from the beginning. In particular, the 0-state corresponds to horizontal polarization and the 1-state to vertical polarization.

We describe below the working principles of each individual operation for a more complete explanation.

It is to be understood that the above phase shifts can all (or in part) set to zero, and therefore there will be a device with a reduced number of components.

<u>Inversion operation</u>

This operation can be directly implemented via application of a “swap” operation on the states:

$$|z\rangle = \frac{z|H\rangle + |V\rangle}{\sqrt{1+|z|^2}} \xrightarrow{swap} \frac{|H\rangle + z|V\rangle}{\sqrt{1+|z|^2}} = \frac{\frac{1}{z}|H\rangle + |V\rangle}{\sqrt{1+\left|\frac{1}{z}\right|^2}} = \left|\frac{1}{z}\right\rangle$$

When exploiting the polarization degree of freedom, as depicted in Figure 3(a), the Inversion operation can be implemented by using a half wave-plate with an optical axis rotated by an angle of π/4 with respect to the horizontal plane (another implementation could be a liquid crystal). This corresponds to the application of the “swap” operation in the polarization degree of freedom. This operation is performed with success probability equal to 1.

Product operation

The product operation between two states is defined as follows:

$$|z_1\rangle|z_2\rangle \xrightarrow{product} |z_1 z_2\rangle$$

This operation is obtained by injecting the two photons in the two input ports of a polarizing beam splitter (see Figure 3(b)) after applications of input phase shifts $(\varphi_{1H}, \varphi_{1V})$ and $(\varphi_{2H}, \varphi_{2V})$. The scheme operates in post-selection, and thus we accept only the events in which the two photons exit from the different output ports of the first PBS. After that, we apply a half-wave plate with an optical axis rotated by an angle of π/8 with respect to the horizontal direction, we apply the two phase-shifts (χ_{3H}, χ_{3V}), and we measure the polarization of the second photon. If the polarization is $|V\rangle$ (corresponding to output marked as “+”) the output state is the product ($|z_1 z_2\rangle$) of the inputs. Conversely, if the polarization is $|H\rangle$ (corresponding to the output marked as “-”) the output state is anti-product ($|-z_1 z_2\rangle$) of the inputs. In principle, one can renounce one of the outputs + or -, and the method works in the same way but with a reduced probability of success for the single operation. One can always obtain one of the two product results by adding an operation with probability equal to 1 (from product to anti-product and vice versa). The correct operation, reproducing the action of transformation $U_{product}$, is obtained when the phase shift values are respectively $\varphi_{1H} = \phi_1 + \phi_2 - \phi_3$, $\varphi_{1V} = \phi_2 + \pi/2$, $\varphi_{2H} = \phi_3 + \pi/2$, $\varphi_{2V} = \phi_1$, $\chi_{3H} = -\phi_2 - \phi_3 - \phi_4$. Phase shift χ_{3V} is redundant, and is thus set to $\chi_{3V} = 0$.

Since this operation is conditioned on the measurement of the polarization state of one of the two photons, we can express the success probability of the product as

$$P_+ = P_- = \frac{1 + |z_1|^2 |z_2|^2}{2(1 + |z_1|^2)(1 + |z_2|^2)}$$

The probability of success is found to be within the range $[0, 0.5]$ and is > 0 everywhere except for the pair of states $(|0\rangle, |\infty\rangle)$ and $(|\infty\rangle, |0\rangle)$. In fact, $0 \times \infty$ is a special case for which the product is indeterminate.

<u>Addition/Sum operation</u>

The arithmetic sum operation between two states is defined as follows

$$|z_1\rangle|z_2\rangle \xrightarrow{sum} |z_1 + z_2\rangle$$

The sum operation, or alternatively the arithmetic mean, is shown in Figure 3. In particular, the two input photons are injected in the two input ports of a partially-polarizing beam-splitter after a set of phase shifts $(\varphi_{1H}, \varphi_{1V}, \varphi_{2H}, \varphi_{2V})$, different for the horizontal and vertical polarization states, is applied. The requested operation is performed when the two photons exit from different outputs of the PPBS. A second set of phase shifts $(\chi_{0H}, \chi_{0V}, \chi_{3H}, \chi_{3V})$, different for the horizontal and vertical polarization states, is then applied on the two output photons. Then, a polarizing beam-splitter is inserted to measure the polarization state of one of the photons. Depending on the outcome, the system performs two different operations.

More specifically, the sum (the arithmetic mean) is obtained when the measured photon is found in the $|V\rangle$ polarization state (corresponding to the outcome marked as "S"), while the harmonic mean, $|z_1\rangle|z_2\rangle \xrightarrow{harmonic\ mean} \left|\frac{z_1 z_2}{z_1+z_2}\right\rangle$, is obtained when the measured photon is found in the $|H\rangle$ polarization state (corresponding to the outcome marked as "I"). The correct operation, reproducing the action of transformation U_{sum}, is obtained when the reflectivities of the PPBS for the two polarizations are respectively $R_H = \frac{5-\sqrt{5}}{10}$ and $R_V = \frac{5+\sqrt{5}}{10}$, while the phase shifts are $\varphi_{1H} = \phi_1 + \pi$, $\varphi_{1V} = \phi_2 + \pi$, $\varphi_{2H} = -\phi_2 - \phi_4$, $\varphi_{2V} = -\phi_1 - \phi_4$, $\chi_{0V} = \phi_1 + \phi_2 + \phi_4$ and $\chi_{3H} = -\phi_1 - \phi_2 - \phi_3 + \pi$. The two phase-shifts χ_{0H} and χ_{3V} are redundant, and are thus set to $\chi_{0H} = 0$ and $\chi_{3V} = 0$. The success probabilities of the two operations are given by the following expressions:

$$P_S = \frac{|z_1 + z_2|^2 + 1}{5(1 + |z_1|^2)(1 + |z_2|^2)}$$

and

$$P_I = \frac{|z_1 + z_2|^2 + |z_1 z_2|^2}{5(1 + |z_1|^2)(1 + |z_2|^2)}$$

Both success probabilities belong to the range $[0, 0.25]$ and are > 0 everywhere except for the states $(|\infty\rangle, |\infty\rangle)$ for the sum and $(|0\rangle, |0\rangle)$ for the harmonic mean, for which the two operations are indeterminate.

<u>Concatenation</u>

The scheme described above can be concatenated to obtain an arbitrary sequence of operations. This can be done by taking the output of a specific step and using it as the input of the subsequent step. For example, the operation $z = z_1 + z_2 + z_3$ is performed by the following steps:

(i) prepare two qubits in the states $|z_1\rangle, |z_2\rangle$

(ii) perform the sum of z_1 and z_2 via the building block described above, which generates one qubit in the photon state $|z_1 + z_2\rangle$

(iii) prepare a third qubit in the state $|z_3\rangle$

(iv) perform the sum between $|z_1 + z_2\rangle$ from the output of step (ii), and $|z_3\rangle$.

The same approach can be applied to arbitrary combinations thanks to the independence of the building blocks from the state of the qubits to be processed. In general, the success probability for an arbitrary concatenation of k operations will be the product of the individual success probabilities of each operation. Furthermore, additional qubits should be prepared for each product/sum operation included in the chain, since the sum and the product consume one qubit (as one photon is absorbed by a photodetector).

Time photonic operations

In this encoding, the two quantum levels correspond to two different pulses separated by a time T greater than the coherence time of the photons. For an electromagnetic wave, the coherence time is the time over which a propagating wave (especially a laser or maser beam) may be considered coherent, meaning that its phase is, on average, predictable. In long-distance transmission systems, the coherence time may be reduced by propagation factors such as dispersion, scattering, and diffraction (the coherence time is set to be equal for the two photons). This condition on T is necessary to ensure that the two states encoded in the pulses at time T_1 and T_2 individuate a two-level system for qubits. To carry out the operations necessary to implement a Bernoulli factory in this degree of freedom, it is possible to make use of a converter from time encoding to polarization encoding and vice versa. This allows us to use the polarization-encoded operations described above.

The time-polarization encoder and decoder are shown in Figure 4. The time-encoded state enters the upper branch of the interferometer where an electro-optical modulator (EOM) applies a bias rotation only on the second pulse (see Figure 4(a)). This operation allows the division of the two pulses after the first polarizing beam-splitter. The first pulse is reflected on the upper branch of the interferometer while the second pulse is transmitted on the lower branch of the interferometer. A delay line (DL) applied to the upper branch synchronizes the two pulses, i.e. compensates for the time interval T between the two pulses. The second polarizing beam-splitter combines together the two pulses which will be synchronized but with orthogonal polarization states. The reverse operation is performed by the interferometer shown in Figure 4(b).

Path-photonic operations

Path encoding was the one investigated for the realization of a MOQBEF prototype according to the present disclosure. More specifically, in this encoding the two quantum levels correspond to the presence of a photon in one of two different paths. As an example, in Figure 5(a) the logical state $|0_L\rangle$ corresponds to the presence of a single photon in the upper mode, and conversely logical state $|1_L\rangle$ corresponds to a single photon in the lower mode. Such an encoding is the optimal choice for information processing on compact devices such as integrated reprogrammable photonic chips. In particular, the path degree of freedom is particularly suitable when using integrated optics, making it easier to implement larger and stable interferometers.

The details of the optical elements necessary to perform the three elementary operations of the MOQBEF on the paths are reported in detail in Figure 5. The input ports of the interferometers are labelled 1 and 2, with outputs labelled *out*. In block (a), Inversion is performed deterministically by swapping the dual-rail modes. In block (b), the product is performed by applying a set of input phase shifts $(\varphi_1, \varphi_2, \varphi_3, \varphi_4)$, by sending component $|1_L\rangle$ of dual-rail qubit 1 (dual-rail because it encodes two states) and component $|0_L\rangle$ of dual-rail qubit 2 into a balanced beam-splitter, by applying a set of phase shifts (χ_2, χ_3) on the output ports of the beam-splitter, and post-selecting events with one of the two photons in output ports - or + in the figure (success determination as in previous embodiment). The state prepared by this measured event is encoded in an output dual-rail qubit labelled *out*. In block (c), the sum is implemented by swapping the input mode component $|1_L\rangle$ of dual-rail qubit 1 and component $|0_L\rangle$ of dual-rail qubit 2, by applying a set of phase shifts $(\varphi_1, \varphi_2, \varphi_3, \varphi_4)$ on the input components of the qubits, by directing the modes in the input ports of two beam-splitters, and by applying a second set of phase shifts $(\chi_1, \chi_2, \chi_3, \chi_4)$. Here, too, the operation is successful when a photon is detected by the detector labelled “S”. The success operation is exactly the same of the implementation of Figure 2.

We describe below the working principles of this approach.

It is to be understood that the above phase shifts can all (or in part) set to zero, and therefore there will be a device with a reduced number of components, except for a few phases that will be specified below.

Inversion operation

To implement the inversion we use the operation implemented by exchanging the modes in the interferometer, as in Figure 5(a). It corresponds to a direct swap of the optical modes. Analogously to the case of polarization encoding, this operation can be carried out deterministically without any qubit measurement and thus the success probability is 1.

Product operation

The block scheme presented in Figure 5(b) implements the product operation between two qubits. First, a set of input phase shifts $(\varphi_1, \varphi_2, \varphi_3, \varphi_4)$, is applied on the input modes. The two modes representing the level $|1_L\rangle_1$ of qubit 1 and the level $|0_L\rangle_2$ of qubit 2 are coupled to the two input ports of a balanced beam-splitter. After applying two phase shifts (χ_2, χ_3), the two output ports of this element are measured with single-photon detectors as shown in the Figure ("+" and "-"). The final state of the qubit encoded in the remaining two modes, depends on the presence of a single photon in one of the two outputs of the beam-splitter. The correct operation, reproducing the action of transformation $U_{product}$, is obtained when the phase shift values are respectively $\varphi_1 = \phi_1 + \phi_2 - \phi_3$, $\varphi_2 = \phi_2$, $\varphi_3 = \phi_3$, $\varphi_4 = \phi_1$, $\chi_3 = -\phi_2 - \phi_3 - \phi_4$. Phase shift χ_2 is redundant and is thus set to $\chi_2 = 0$.

Here, the minimal set of phase shift is with $\varphi_1 = \pi$ and the others set to zero. The expression of the output qubit is:

$$|z_1 z_2\rangle_{out} = \frac{\pm z_1 z_2 |0_L\rangle_{out} + |1_L\rangle_{out}}{\sqrt{1 + |z_1 z_2|^2}}$$

where the sign $\pm$ will depend on which detector signals the presence of a photon. The success probabilities associated to the operations are given by:

$$P_+ = P_- = \frac{1 + |z_1|^2 |z_2|^2}{2(1 + |z_1|^2)(1 + |z_2|^2)}$$

The probability of success is found to be within the range $[0, 0.5]$ and is > 0 everywhere except for the pair of states $(|0\rangle, |\infty\rangle)$ and $(|\infty\rangle, |0\rangle)$, for which the product operation is indeterminate.

<u>Addition/sum operation</u>

The interferometer of Figure 5(c) implements the sum operation between two qubits. First, the modes corresponding to level $|1_L\rangle_1$ of qubit 1 and level $|0_L\rangle_2$ of qubit 2 are swapped. Then, a set of phase shifts $(\varphi_1, \varphi_2, \varphi_3, \varphi_4)$, is applied on the modes. The two photons are injected into the interferometer and two identical beam splitters are used to couple the qubit levels according to the scheme of Figure 5(c). After the mixing process, a second set of phase shifts $(\chi_1, \chi_2, \chi_3, \chi_4)$, is applied on the modes, and one output port of each beam-splitter is measured. The correct operation, reproducing the action of transformation U_{sum}, is obtained when the phase shift values are respectively $\varphi_1 = \phi_1$, $\varphi_2 = \phi_2$, $\varphi_3 = -\phi_2 - \phi_4$, $\varphi_4 = -\phi_1 - \phi_4$, $\chi_2 = -\phi_1 - \phi_2 - \phi_3$ and $\chi_2 = +\phi_1 + \phi_2 + \phi_4$. Phase shifts χ_1 and χ_3 are redundant and are thus set to $\chi_1 = 0$ and $\chi_3 = 0$. The sum operation is performed when one photon is detected at the output marked as “S”.

Here, the minimal set of phase shift is with $\chi_4 = \pi$ and the others set to zero. The state of the sum qubit is:

$$|S\rangle_{out} = \frac{(z_1 + z_2)\frac{\sqrt{RT}}{R - T}|0_L\rangle_{out} + |1_L\rangle_{out}}{c}$$

where R and T are the reflectivity and transmissivity of the beamsplitters, and c is the normalization factor. Conversely, if the photon is detected on the output marked as “I”, the harmonic mean operation is performed, and the corresponding state is:

$$|I\rangle_{out} = \frac{-\frac{z_1 z_2}{z_1 + z_1}\frac{R - T}{\sqrt{RT}}|0_L\rangle_{out} + |1_L\rangle_{out}}{c}$$

To obtain the output qubit in the sum or harmonic mean state, we observe that the multiplicative factor c is a real number and can be set to 1 when the reflectivity of both beamsplitters is $R = \frac{5+\sqrt{5}}{10}$. With this value of the reflectivity, the probability to detect one photon in “S” is then given by:

$$P_S = \frac{|z_1 + z_2|^2 + 1}{5(1 + |z_1|^2)(1 + |z_2|^2)}$$

It represents the success probability of the sum operation. The probability to find one photon in “I” is given by:

$$P_I = \frac{|z_1 + z_2|^2 + |z_1 z_2|^2}{5(1 + |z_1|^2)(1 + |z_2|^2)}$$

The success probability is > 0 everywhere except for the states $(|\infty\rangle, |\infty\rangle)$ and $(|0\rangle, |0\rangle)$ for which the sum and the harmonic mean are indeterminate respectively.

Orbital angular momentum operations

In this encoding, the two quantum levels correspond to two different eigenstates of the orbital angular momentum (OAM) operator of the electromagnetic field. Examples of such states are the Laguerre Gauss (LG) modes, a family of solutions of the Helmholtz equation. A light beam that carries OAM means that has an helicoidal wavefront. The value of OAM corresponds to the windings number of the optical phase of the wavefront in the transverse plane. The OAM can assume only integer values. Then, a qubit state is encoded by considering two different values m_1 and m_2 of the OAM. To carry out the operations necessary to implement a Bernoulli factory in this degree of freedom, it is possible to make use of a converter from OAM encoding and path encoding and vice versa. This allows us to use the path-encoded operations described above.

The OAM-path encoder and decoder, shown schematically in Figure 6, are based on a device called OAM-sorter. The OAM-sorter displaces the two states $|m_1\rangle = |0_L\rangle$ and $|m_2\rangle = |1_L\rangle$ in two separated paths, thus converting an OAM-based qubit into a path-encoded qubit. An example of such a device can be found in Ref. [16]. The reverse operation is performed by another OAM-sorter that takes as input the path photonic qubit such as the output of the path-encoded MOQBEF and converts the information in the OAM logical states.

In other words, the respective qubits in the first photon and the second photon are encoded in their orbital angular momentum, OAM as follows:

- a first OAM-sorter for the first photon qubit and a second OAM-sorter for the second photon qubit are provided and configured to convert the OAM-based qubits into path-encoded qubits;
- the multiplication interferometer and the sum interferometer as above described are provided, which take as inputs the path-encoded qubits;
- a third OAM sorter is provided and configured to convert the output path-encoded qubit of step B into OAM-based qubit as follows:
  - the third OAM-sorter is configured to take the output modes from the multiplication interferometer as inputs;
  - the third OAM-sorter is configured to take the output modes from the sum interferometer as inputs.

<u>Operations in the frequency domain</u>

In the frequency bins encoding, the two quantum levels are two well separated optical frequencies ω_1 and ω_2. The difference $\Delta\omega$ between them is greater than the spectral width of the two individual frequencies. For simplicity, we can consider two states as monochromatic waves for which the spectral width is negligible. These conditions on $\Delta\omega$, ω_1 and ω_2 are necessary to ensure that the two states encoded in the two frequencies individuate a two-level system for qubits. To carry out the operations necessary to implement a Bernoulli factory in this degree of freedom, it is possible to make use of a converter from frequency-bin encoding and path encoding and vice versa. This allows us to use the path-encoded operations described above.

The frequency-path encoder and decoder, shown schematically in Figure 7, are based on a device able to mix different frequency components ω_1 and ω_2. Encoding can be performed by separating the different frequency components in two separate spatial modes via a wavelength demultiplexer (WD). Then a beam-splitter operation with transmittivity $T = 0.5$ is performed between the frequency components on each spatial mode. Such a beam-splitter operation can be performed with a scheme called quantum frequency processor (QFP) described in Ref. [17]. Finally, the conversion is completed by further separating the components with different frequencies and post-selecting on the output ports corresponding to the same frequency. The reverse scheme can be used to perform in a post-selected configuration the inverse operation, that is, decoding from path to frequency.

More in detail, the qubit in the first photon is encoded as a first and a second frequency state, wherein the difference between the two frequencies is greater than the spectral width of each of the two frequencies, and the qubit in the second photon is encoded using the first and the second frequency, and:

- a first converter is provided and configured to convert the first photon qubit into a first path-encoded qubit, and a second converter is provided and configured to convert the second photon qubit into a second path-encoded qubit, wherein each of the first and second converter includes a first wavelength demultiplexer (WD) configured to separate the first and second frequency states, and a beam-splitter is provided and configured with transmittivity $T = 0.5$ between the frequency states at the output of the first and second converter, and a respective second and third wavelength demultiplexers (WD) having each two output ports are provided and configured to separate the two frequency states on each mode, and finally separation means are provided and configured to select on the two output ports of each second and third wavelength demultiplexer (WD) the modes corresponding to a same frequency between the first and second frequency, thus obtaining corresponding path-encoded qubits;

- the multiplication interferometer and the sum interferometer as above described are provided, which take as inputs the path-encoded qubits;
- a third converter with two input ports is provided and configured to convert the multiplication photon or sum photon into respective frequency-encoded qubits, wherein a beam-splitter with transmittivity $T = 0.5$ between the frequency states is provided and configured which takes as input the multiplication photon or sum photon, and a respective fourth and fifth wavelength demultiplexer (WD) having each two output ports is provided and configured to separate the two frequency states on each mode of the multiplication or sum photon from the beam splitter, and then a sixth demultiplexer having an only output port is provided and configured to recombine the output modes with different frequencies from the fourth and fifth demultiplexers (at the only output port the photon is in an only spatial mode with two frequency components).

Prototype

We now describe in more detail the characteristics of a prototype composed of an integrated interferometer which allows for the implementation of the MOQBEF in the path encoding which operates on 3 qubits. The device shown in Figure 8(a) was fabricated via the femtosecond-laser-writing technique. The strong pulsed laser focused on a silica sample directly writes the waveguides, which result from a permanent change of the refractive index of the material.

The circuit is a network of tunable beam-splitters and phase shifters shown in Figure 8(a). The reflectivity of such tunable beam-splitters is controlled and reprogrammable by the use of an external resistor placed on the sample surface. By applying a voltage, the heat produced by the Joule effect will locally modify the refractive index of the underlying guides. In this way it is possible to control not only the reflectivities of the beam-splitters but also the phase relationships (the rectangles in the Figure) between the various paths. The circuit therefore allows to concatenate up to two operations of sum and product and to encode 3 photonic qubits. We recall that the operations of addition and product require the measurement of one photon each. Therefore, this scheme that processes up to 3 photonic qubits can concatenate up to two operations of type sum and/or product.

The integrated device (Figure 8(a)) has six input and output modes and 30 resistors which allow the parameters of the optical circuit to be controlled by the thermo-optic effect. They control the reflectivities of the beam-splitters in Figure 8(a), as well as the phase shifters represented by rectangles in the schematic. The beam-splitters with tunable beam-splitting ratios are actually implemented via a Mach-Zehnder interferometer featuring two 50/50 beam-splitters and a phase shifter in between (Figure 8 (b)).

We describe below in detail the different scheme for the implementation of the building blocks, and the concatenations of two of them, with a 6-mode device having the structure reported in Figure 8.

Building blocks

The product and addition/sum operations can be implemented by appropriately programming the above device. In greater detail, one can use a beam splitter with the capability of changing its reflectivity (r in Figure 8 (ab)) followed by a phase shifter in one of the paths.

Practically, the circuit programming can be performed by replacing the above beam splitter with a sequence of two identical fixed beam splitters (right hand side of Figure 8 (b)) each with a phase shifter on one path.

When working with optical integrated circuits, one can use thermal phase shifters to change the phase acquired by light propagation in a waveguide.

In order to realize sum and product operations, some of the beam-splitters of Figure 8(a) are programmed as identity or swap operation that corresponds to the inversion.

A detailed exemplary structure of how to program the devices is reported in Figure 9(a) for the product operation. In this case, the input photons are injected in ports 3-4 (first qubit) and ports 5-6 (second qubit). The scheme then requires two photons, and ports 1-2 are not used for this single operation.

In Figure 9(b) we further show the scheme for the addition/sum operation. The input photons are injected in this case in input ports 1-2 (first qubit) and 3-4 (second qubit), while in case the unused ports are 5-6. We note that the final step shown in Figure 9 (marked as “State Tomography") is not part of the protocol. Indeed, it is an additional step that can be used to measure and analyze the output of the MOQBEF. If this step is not required (as for example when using the output as an input of another algorithm, the state tomography being only a verification step), and the output needs to be reused for additional processing, all beam-splitters can be set to act as the identity.

In the Figure, the “State preparation” block is a standard means for the preparation of the input photons and as such it is not a part of the disclosure.

Concatenation of two operations

As an example, we show in Figure 10 the configuration of the interferometer which leads to the concatenation of one product and one addition operation. More specifically, we show in Figure 10(a) a specific configuration that implements the case $|z_1\rangle|z_2\rangle|z_3\rangle \rightarrow|z_4\rangle = |(z_1 + z_2)z_3\rangle$ (the output qubit is found at ports 4-5, when the other two photons are detected in the output mode pairs (1,2), (3,6)).

Conversely, Figure 10(a) shows a specific configuration corresponding to the case $|z_1\rangle|z_2\rangle|z_3\rangle \rightarrow|z_4\rangle = |z_1 z_2 + z_3\rangle$ (The output qubit is encoded in the modes 3-4 when the other two photons are detected in the mode pairs (1,5), (2,6)). In both cases, all input ports are used, and three input photons are required.

Concatenation, modularity and scalability

Starting from the schemes discussed above, the MOQBEF method presents relevant properties for the extension to larger instances. As discussed, crucial requirements are indeed the possibility of implementing arbitrary elementary operations, with a modular approach which requires only replicating sequences of elementary operations. Furthermore, it must require a scalable hardware implementation, also in terms of long-term stability. Our MOQBEF satisfies these requirements, thus renders this scheme suitable for adoption in different scenarios beyond those discussed in this document. More specifically, we emphasize that:

(i) concatenation of arbitrary sequences is possible according to the discussion above;

(ii) the modularity of the approach allows to generalize everything to the n-qubit scenario by replicating the concatenations of the elementary operations;

(iii) scalability is guaranteed by the compactness and stability of the integrated platforms.

As an example of the above, a MOQBEF at 5 qubits is schematized in Figure 11. The MOQBEF acts on 5 dual-rail path encoded qubits. This photonic circuit implements the following function: $|z\rangle = |z_1 z_2 z_3 + z_4 z_5\rangle$.

Bibliography

[1] M. S. Keane and G. L. O'Brien, ACM Trans. Model. Comput. Simul. 4, 2139 (1994).
[2] D. Vats, F B Gonçalves, K. Łatuszynski, and G. O. Roberts, Volume 109, Issue 2, June 2022, Pages 369–385 Biometrika (2021).
[3] S. Dughmi, J. D. Hartline, R. Kleinberg, and R. Niazadeh, ACM SIGecom Exchanges 16, 58 (2017).
[4] J. M. Flegal. R. Herbei. "Exact sampling for intractable probability distributions via a Bernoulli factory." Electron. J. Statist. 6 10 - 37, 2012. https://doi.org/10.1214/11-EJS663
[5] R. Herbei, and L. M. Berliner, Estimating ocean circulation: an MCMC approach with approximated likelihoods via the Bernoulli factory. J. Amer. Statist. Assoc. 109 944–954 (2014).
[6] Y. Cai, A. Oikonomou, G. Velegkas, and M. Zhao, (2019), An Efficient ε-BIC to BIC Transformation and Its Application to Black-Box Reduction in Revenue Maximization. arXiv preprint arXiv:1911.10172.
[7] H. Dale, D. Jennings, and T. Rudolph, Nature Communications 6, Article number: 8203 (2015).
[8] H. Dale, "Quantum coins and quantum sampling," Electronic Thesis or Diss., Imperial College London, 2016. http://hdl.handle.net/10044/1/49203. (2016).
[9] X. Yuan, K. Liu, Y. Xu, W. Wang, Y. Ma, F. Zhang, Z. Yan, R. Vijay, L. Sun, and X. Ma, Phys. Rev. Lett. 117, 010502 (2016).
[10] R. B. Patel, T. Rudolph, and G. J. Pryde, Science Advances 5, eaau6668 (2019).
[11] J. Jiang, J. Zhang, and X. Sun, Physical Review A 97 (2018).

[12] Y. Liu, J. Jiang, P. Zhu, D. Wang, J. Ding, X. Qiang, A. Huang, P. Xu, J. Zhang, G. Tian, X. Fu, M. Deng, C. Wu, X. Sun, X. Yang, and J. Wu, Quantum Science and Technology 6, 045025 (2021).
[13] X. Zhan, K. Wang, L. Xiao, Z. Bian, and P. Xue, Phys. Rev. A 102, 012605 (2020).
[14] A. Broadbent, J. Fitzsimons, E. Kashefi, 50th Annual IEEE Symposium on Foundations of Computer Science, pp. 517–526 (2009)
[15] J. B. Bronzan, Physical Review D 38, 1994 (1988).
[16] N. K. Fontaine, R. Ryf, H. Chen, D. T. Neilson, K. Kim, J. Carpenter, Nature Communications 10, Article number: 1865 (2019).
[17] H.-H. Lu, E. M. Simmerman, P. Lougovski, A. M. Weiner, J. M. Lukens, Physical Review Lettes 125, 120503 (2020).

In the foregoing the preferred embodiments have been described and variants of the present invention have been suggested, but it should be understood that those skilled in the art will be able to make modifications and changes without thereby departing from the relative scope of protection, as defined by the attached claims.

CLAIMS

1. Method for the application of concatenable elementary arithmetic operations to photonic qubits, wherein each qubit has two states or modes encoded in a single photon, wherein the states or modes are $|0_L\rangle$ and $|1_L\rangle$, and the following steps are executed:

A. producing a first and second single photons each encoding corresponding qubits $|z_1\rangle$ and $|z_2\rangle$;

The method being characterized in that the following further steps are executed:

B. applying one of said concatenable elementary arithmetic operations by:

B1. in the case of multiplication operation, inputting the first photon encoding qubit $|z_1\rangle$ and the second photon encoding qubit $|z_2\rangle$ into a multiplication interferometer, the multiplication interferometer being configured to perform the transformation $|z_1\rangle,|z_2\rangle \rightarrow |z_1 z_2\rangle$, and wherein the first photon is provided as multiplication photon at a first output of the interferometer, and the second photon $|z_2\rangle$ is measured at a first sub-output or at a second sub-output of the multiplication interferometer, the output photon at the first output being taken as encoding the product $|z_1 z_2\rangle$ when the second photon is detected at the first sub-output only or as encoding the anti-product $|-z_1 z_2\rangle$ when the second photon is detected at the second sub-output only, wherein the multiplication interferometer is configured to realize the following unitary transformation $U_{product}$ on the four modes of the first and second photon:

$$\begin{pmatrix} e^{i(\phi_1+\phi_2-\phi_3)} & 0 & 0 & 0 \\ 0 & -\frac{e^{i\phi_2}}{\sqrt{2}} & \frac{e^{i\phi_3}}{\sqrt{2}} & 0 \\ 0 & \frac{e^{-i(\phi_3+\phi_4)}}{\sqrt{2}} & \frac{e^{-i(\phi_2+\phi_4)}}{\sqrt{2}} & 0 \\ 0 & 0 & 0 & e^{i\phi_1} \end{pmatrix},$$

Wherein parameters ϕ_1, ϕ_2, ϕ_3, ϕ_4 can take any value between 0 and 2π; or

B2. in the case of sum operation, inputting the first photon encoding qubit $|z_1\rangle$ and the second photon encoding qubit $|z_2\rangle$ into a sum interferometer configured to perform the transformation $|z_1\rangle,|z_2\rangle \rightarrow |z_1+z_2\rangle$ wherein the first photon is provided at a first output of the sum interferometer as sum photon, and the second photon $|z_2\rangle$ is measured at a first sub-output or at a second sub-output of the sum interferometer, the first photon at the first output being taken as encoding the sum $|z_1+z_2\rangle$ when the second photon is detected at the first sub-output only or as encoding the harmonic mean $\left|\frac{z_1 z_2}{z_1+z_2}\right\rangle$ when the second photon is detected at the second sub-output only, wherein the sum interferometer is configured to realize the following unitary transformation U_{sum} on the four modes of the first and second photon:

$$\begin{pmatrix} -\sqrt{\frac{5+\sqrt{5}}{10}}e^{i\phi_1} & 0 & \sqrt{\frac{5-\sqrt{5}}{10}}e^{i\phi_2} & 0 \\ \sqrt{\frac{5-\sqrt{5}}{10}}e^{-i(\phi_2+\phi_3)} & 0 & \sqrt{\frac{5+\sqrt{5}}{10}}e^{-i(\phi_1+\phi_3)} & 0 \\ 0 & -\sqrt{\frac{5+\sqrt{5}}{10}}e^{-i(\phi_2+\phi_4)} & i\sqrt{\frac{5+\sqrt{5}}{10}} & \sqrt{\frac{5-\sqrt{5}}{10}}e^{-i(\phi_1+\phi_4)} \\ 0 & \sqrt{\frac{5-\sqrt{5}}{10}}e^{i\phi_1} & 0 & \sqrt{\frac{5+\sqrt{5}}{10}}e^{i\phi_2} \end{pmatrix},$$

Wherein parameters ϕ_1, ϕ_2, ϕ_3, ϕ_4 can take any value between 0 and 2π.

2. Method according to claim 1, wherein qubit $|z_1\rangle$ or $|z_2\rangle$, their sum or product undergoes an inversion operation in a step B3, by making the corresponding photon propagate through an inversion optical device configured to perform the transformation $|z\rangle \rightarrow |1/z\rangle$ and output an inverted modes photon, wherein the inversion optical device is configured to realize the following unitary transformation on the two modes:

$$U_{inversion} = \begin{pmatrix} 0 & 1 \\ 1 & 0 \end{pmatrix}.$$

3. Method according to claim 2, wherein in the product or sum interferometer, or in the inversion optical device the following is provided:

- at the input, additional empty modes inputs, wherein no photons are injected;
- at the output, additional empty modes outputs corresponding to the additional empty modes inputs, wherein the additional empty modes outputs are discarded;

the sum, product or inversion transformation being a unitary matrix U in a mode space enlarged with the additional empty modes outputs and the additional empty modes inputs.

4. Method according to any one claim 1 to 3, wherein the qubits in the first photon and the second photon are encoded in their polarization, and the elementary arithmetic operations are implemented as follows:

- in step B1, the first and second photon are injected into and then separated by a Polarizing Beam Splitter, the second photon being made propagate through a half-wave plate or a liquid crystal and then through a further Polarizing Beam Splitter whose outputs are said two sub-outputs;
- in step B2, the first and second photon are injected into two input ports of a partially-polarizing Beam Splitter and the result is selected when the first and second photons exit from different output ports of the partially-polarizing Beam Splitter, the second

photon being then made propagate through a further polarizing Beam Splitter, whose outputs are said two sub-outputs.

5. Method according to claim 2 and 4, wherein in step B3 the single photon is made pass through a half-wave plate or a liquid crystal.

6. Method according to claim 4 or 5, wherein the qubits in the first photon and the second photon are encoded as pulses at time T_1 and T_2 of an electromagnetic wave, wherein $|T_1-T_2|$ is greater than the coherence time of the first and second photon, and wherein a time-polarization encoder is used before injecting the two photons into the interferometer or the half wave plate or liquid crystal, and a time-polarization decoder is used at the output of the interferometer to pass from time qubit encoding to polarization qubit encoding and vice versa.

7. Method according to any one claim 1 to 3, wherein the respective qubits in the first photon and the second photon are spatially encoded in their path, and the elementary arithmetic operation are implemented as follows:

- in step B1:
  - mode $|0_L\rangle$ of the first photon is made propagate through a first waveguide with a phase-shift and mode $|1_L\rangle$ of the second photon is made propagate unaltered through a second waveguide, the outputs modes of the first and second waveguide constituting said multiplication photon;
  - mode $|1_L\rangle$ of the first photon and mode $|0_L\rangle$ of the second photon are made propagate through corresponding waveguides and a balanced Beam Splitter whose outputs are said first and second sub-outputs;
- in step B2:

- mode $|0_L\rangle$ of the first photon and mode $|0_L\rangle$ of the second photon are made propagate through two waveguides through a Beam Splitter with reflectivity $R = \frac{5+\sqrt{5}}{10}$, the two outputs of the Beam Splitter providing mode $|0_L\rangle$ of the sum photon and said first sub-output;
- mode $|1_L\rangle$ of the first photon and mode $|1_L\rangle$ of the second photon are made propagate through two waveguides through a further Beam Splitter with reflectivity $R = \frac{5+\sqrt{5}}{10}$, one output of the further Beam Splitter being followed by a phase-shift and providing mode $|1_L\rangle$ of the sum photon and the other output of the further Beam Splitter providing said second sub-output.

8. Method according to claim 2 and 7, wherein in step B3 each mode of the single photon is made propagate through respective waveguides, wherein the respective waveguides are configured to swap the optical modes of the single photon.

9. Method according to claim 7, wherein the respective qubits in the first photon and the second photon are encoded in their orbital angular momentum, OAM, and:

- a first OAM-sorter for the first photon qubit and a second OAM-sorter for the second photon qubit are used to convert the OAM-based qubits into path-encoded qubits;
- the method of claim 7 is performed on the path-encoded qubits;
- a third OAM sorter is used to convert the output path-encoded qubit of step B into OAM-based qubit as follows:
  - In step B1, the multiplication photon modes are plugged into two input ports of the third OAM sorter;

- In step B2, the sum photon modes are plugged into two input ports of the third OAM sorter.

10. Method according to claim 7, wherein the qubit in the first photon is encoded as a first and a second frequency state, wherein the difference between the two frequencies is greater than the spectral width of each of the two frequencies, and the qubit in the second photon is encoded using the first and the second frequency, and:

- a first converter is used to convert the first photon qubit into a first path-encoded qubit, and a second converter is used to convert the second photon qubit into a second path-encoded qubit, wherein each of the first and second converter includes separating the first and second frequency states via a first wavelength demultiplexer (WD), and then performing a beam-splitter operation with transmittivity $T = 0.5$ between the frequency states, and then further separating the two frequency states on each mode via a respective second and third wavelength demultiplexers (WD) having each two output ports, and finally selecting on the two output ports of each second and third wavelength demultiplexer (WD) the modes corresponding to a same frequency between the first and second frequency, thus obtaining corresponding path-encoded qubits;
- performing the method of claim 7 on the path-encoded qubits;
- using a third converter with two input ports to convert the multiplication photon or sum photon of step B into respective frequency-encoded qubits, by inputting the multiplication photon or sum photon into a beam-splitter with transmittivity $T = 0.5$ between the frequency states, and then further separating the two frequency states on each mode via a respective fourth and fifth wavelength demultiplexers (WD) having each two output ports, and then recombining the output modes with different frequencies of the fourth

and fifth demultiplexers by a sixth demultiplexer having an only output port.

11. Method according to any one claim 1 to 10, wherein the inversion photon, or the multiplication photon or the sum photon are taken as input photon in steps B1 and/or B2 and/or B3, thus realizing a concatenation of said elementary arithmetic operations.

12. Method for realizing a Quantum-to-Quantum Bernoulli Factory, characterized in that random qubits with unknown bias are encoded into corresponding photons and one or more elementary arithmetic operations according to the method of any claim 1 to 11 are applied to the random qubits with unknown bias to obtain random qubits with a predefined bias.

13. Quantum Interferometer, comprising optical means configured to realize concatenable elementary arithmetic operations of photonic qubits, wherein each qubit has two states or modes encoded in a single photon, wherein the states or modes are $|0_L\rangle$ and $|1_L\rangle$, the Quantum Interferometer being characterized in that it comprises:

- a multiplication interferometer with inputs for the first photon encoding qubit $|z_1\rangle$ and the second photon encoding qubit $|z_2\rangle$, the multiplication interferometer being configured to perform the transformation $|z_1\rangle,|z_2\rangle \rightarrow |z_1 z_2\rangle$, and wherein the multiplication interferometer is provided with a first output configured to output the multiplication photon qubit $|z_1 z_2\rangle$, and a first multiplication sub-output and a second multiplication sub-output provided with respective photodetectors and configured to alternatively output the second photon qubit $|z_2\rangle$, wherein the multiplication interferometer is configured to realize the unitary transformation $U_{product}$ defined in claim 1; or

- a sum interferometer with inputs for the first photon encoding qubit $|z_1\rangle$ and the second photon encoding qubit $|z_2\rangle$, the sum interferometer being configured to perform the transformation $|z_1\rangle,|z_2\rangle \rightarrow |z_1 + z_2\rangle$, and wherein a first sum sub-output and a second sum sub-output are provided with respective photodetectors, wherein the first sum sub-output is configured to output the second photon qubit $|z_2\rangle$ or a qubit encoding the harmonic mean $\left|\frac{z_1 z_2}{z_1+z_2}\right\rangle$ when the second photon is detected at the second sum sub-output only, wherein the sum interferometer is configured to realize the unitary transformation U_{sum} defined in claim 1.

14. Quantum Interferometer according to claim 13, wherein the sum or multiplication interferometer is optically connected to an inversion optical device configured to perform a unitary inversion transformation as defined in claim 2.

15. Quantum Interferometer according to claim 13 or 14, wherein the qubits in the first photon and the second photon are encoded in their polarization, and:

- in the multiplication interferometer, the first and second inputs are inputs of a Polarizing Beam Splitter, an output of the Polarizing Beam Splitter being optically connected to a half-wave plate or a liquid crystal, which in turn are optically connected to a further Polarizing Beam Splitter whose outputs are said first and second multiplication sub-outputs;
- in the sum interferometer, the first and second inputs are inputs of a partially-polarizing Beam Splitter, and one output of the partially-polarizing Beam Splitter is optically connected to a further polarizing Beam Splitter, whose outputs are said two first and second sum sub-outputs.

16. Quantum Interferometer according to claim 14 and 15, wherein the inversion optical device is a half-wave plate or a liquid crystal.

17. Quantum Interferometer according to claim 13 or 14, wherein the qubits in the first photon and the second photon are encoded as pulses at time T_1 and T_2 of an electromagnetic wave, wherein $|T_1-T_2|$ is greater than the coherence time of the first and second photon, and wherein a time-polarization encoder is provided just before the inputs of the sum or multiplication interferometer or a half wave plate or liquid crystal, and a time-polarization decoder is used at the outputs of the sum and multiplication interferometer or a half wave plate or liquid crystal, the time-polarization decoder being configured to pass from time qubit encoding to polarization qubit encoding and vice versa.

18. Quantum Interferometer according to claim 13 or 14, wherein the respective qubits in the first photon and the second photon are spatially encoded in their path, and the elementary arithmetic operation are implemented as follows:

- in the multiplication interferometer:
  - a first waveguide is provided, which is configured to make mode $|0_L\rangle$ of the first photon propagate through a first waveguide with a phase-shift and a second waveguide is provided which is configured to make mode $|1_L\rangle$ of the second photon propagate unaltered, till said first multiplication sub-output;
  - corresponding waveguides and a subsequent balanced Beam Splitter are provided, which are configured to make mode $|1_L\rangle$ of the first photon and mode $|0_L\rangle$ of the second

photon propagate till said second multiplication sub-output;

- in the sum interferometer:
  - two sum waveguides and a subsequent Beam Splitter with reflectivity $R = \frac{5+\sqrt{5}}{10}$ are provided which are configured to make mode $|0_L\rangle$ of the first photon and mode $|0_L\rangle$ of the second photon propagate till said first and second sum sub-outputs constituted by the outputs of the Beam Splitter;
  - two different sum waveguides and a further Beam Splitter with reflectivity $R = \frac{5+\sqrt{5}}{10}$ are provided, which are configured to make mode $|1_L\rangle$ of the first photon and mode $|1_L\rangle$ of the second photon propagate, one output of the further Beam Splitter being followed by a phase-shift and providing mode $|1_L\rangle$ as the first sum sub-output and the other output of the further Beam Splitter providing said second sum sub-output.

19. Quantum Interferometer according to claim 16 and 18, wherein in the inversion optical device, respective waveguides are provided which are configured to make each mode of the single photon propagate, wherein the respective waveguides are configured to swap the optical modes of the single photon.

20. Quantum Interferometer according to claim 18, wherein the respective qubits in the first photon and the second photon are encoded in their orbital angular momentum, OAM as follows:

- a first OAM-sorter for the first photon qubit and a second OAM-sorter for the second photon qubit are provided and configured to convert the OAM-based qubits into path-encoded qubits;
- the multiplication interferometer and the sum interferometer of claim 18 are provided, which take as inputs the path-encoded qubits;
- a third OAM sorter is provided and configured to convert the output path-encoded qubit of step B into OAM-based qubit as follows:
  - the third OAM-sorter is configured to take the output modes from the multiplication interferometer as inputs;
  - the third OAM-sorter is configured to take the output modes from the sum interferometer as inputs.

21. Quantum Interferometer according to claim 18, wherein the qubit in the first photon is encoded as a first and a second frequency state, wherein the difference between the two frequencies is greater than the spectral width of each of the two frequencies, and the qubit in the second photon is encoded using the first and the second frequency, and:

- a first converter is provided and configured to convert the first photon qubit into a first path-encoded qubit, and a second converter is provided and configured to convert the second photon qubit into a second path-encoded qubit, wherein each of the first and second converter includes a first wavelength demultiplexer (WD) configured to separate the first and second frequency states, and a beam-splitter is provided and configured with transmittivity $T = 0.5$ between the frequency states at the output of the first and second converter, and a respective second and third wavelength demultiplexers (WD) having each two output ports are provided and configured to separate the two frequency states on each mode, and finally separation means are provided and configured to select on the two output ports of each second and third wavelength demultiplexer (WD) the modes corresponding to a same frequency between the first and second frequency, thus obtaining corresponding path-encoded qubits;

- the multiplication interferometer and the sum interferometer of claim 18 are provided, which take as inputs the path-encoded qubits;
- a third converter with two input ports is provided and configured to convert the multiplication photon or sum photon into respective frequency-encoded qubits, wherein a beam-splitter with transmittivity $T = 0.5$ between the frequency states is provided and configured which takes as input the multiplication photon or sum photon, and a respective fourth and fifth wavelength demultiplexer (WD) having each two output ports is provided and configured to separate the two frequency states on each mode of the multiplication or sum photon from the beam splitter, and then a sixth demultiplexer having an only output port is provided and configured to recombine the output modes with different frequencies from the fourth and fifth demultiplexers.

22. Quantum Interferometer according to any one claim 13 to 21, wherein the multiplication interferometer and/or the sum interferometer and/or the inversion optical device are optically connected in a sequence, thus realizing a concatenation of said elementary operations.

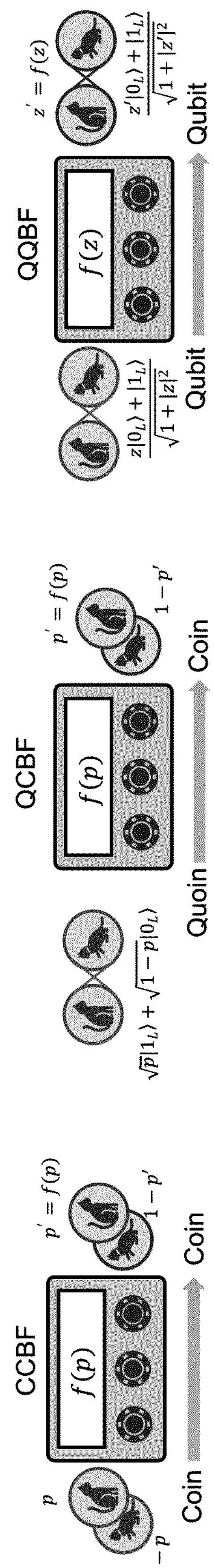

Fig. 1 (PRIOR ART)

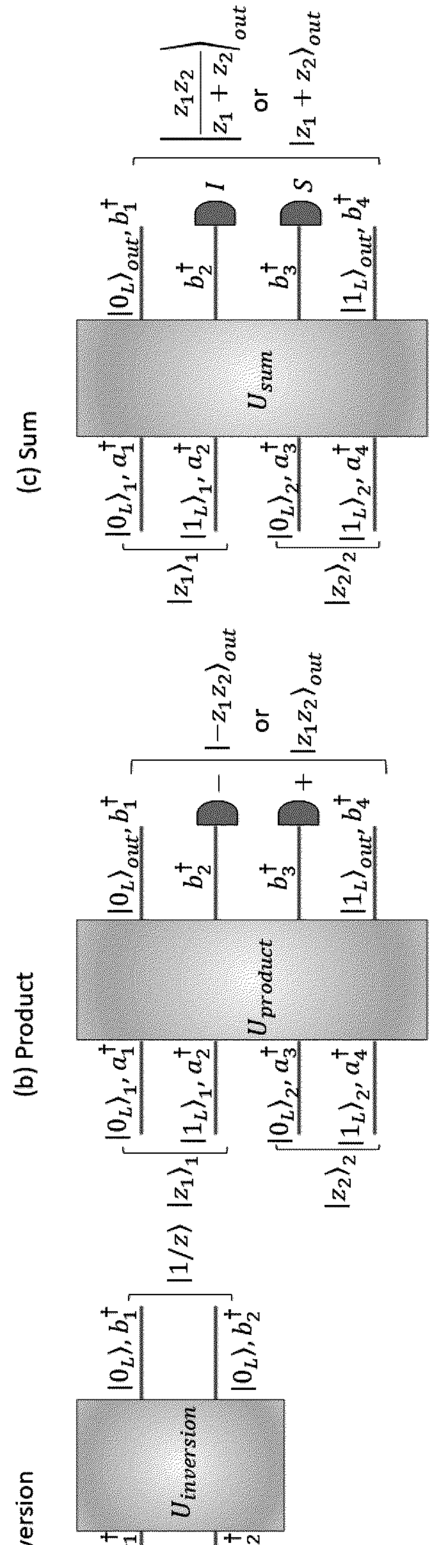

Fig. 2

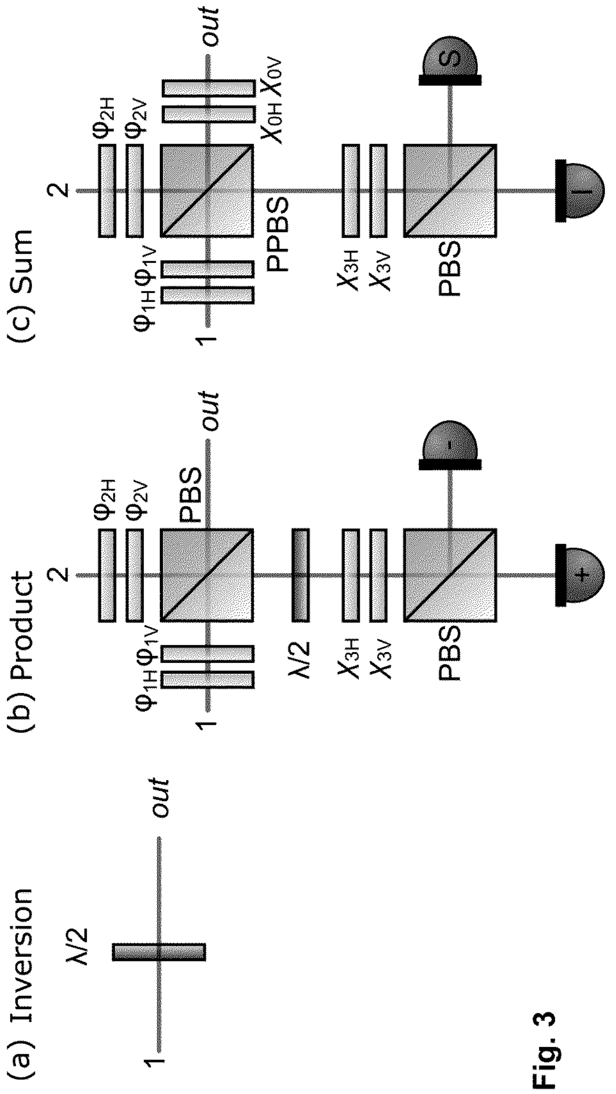
(a) Inversion
λ/2
1
out
(b) Product
φ1H φ1V
φ2H φ2V
1
2
PBS
out
λ/2
X3H X3V
PBS
+
-
(c) Sum
φ1H φ1V
φ2H φ2V
1
2
PPBS
out
X0H X0V
X3H X3V
PBS
I
S

Fig. 3

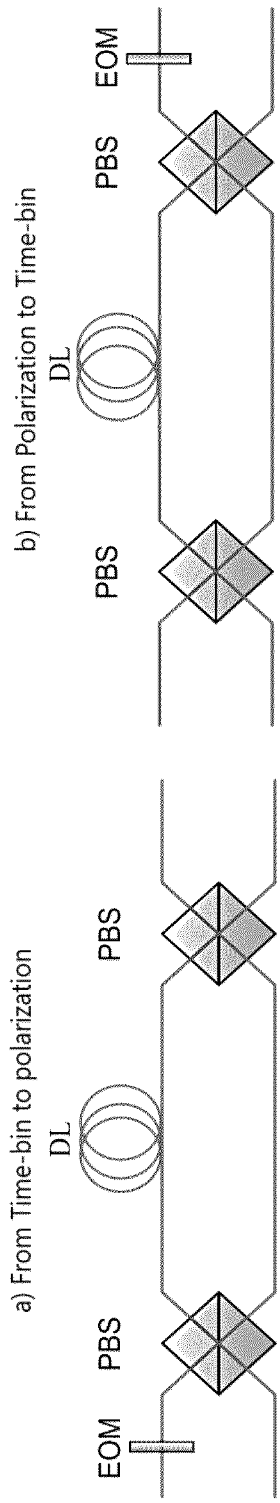
a) From Time-bin to polarization
EOM
PBS
DL
PBS
b) From Polarization to Time-bin
PBS
DL
PBS
EOM

Fig. 4

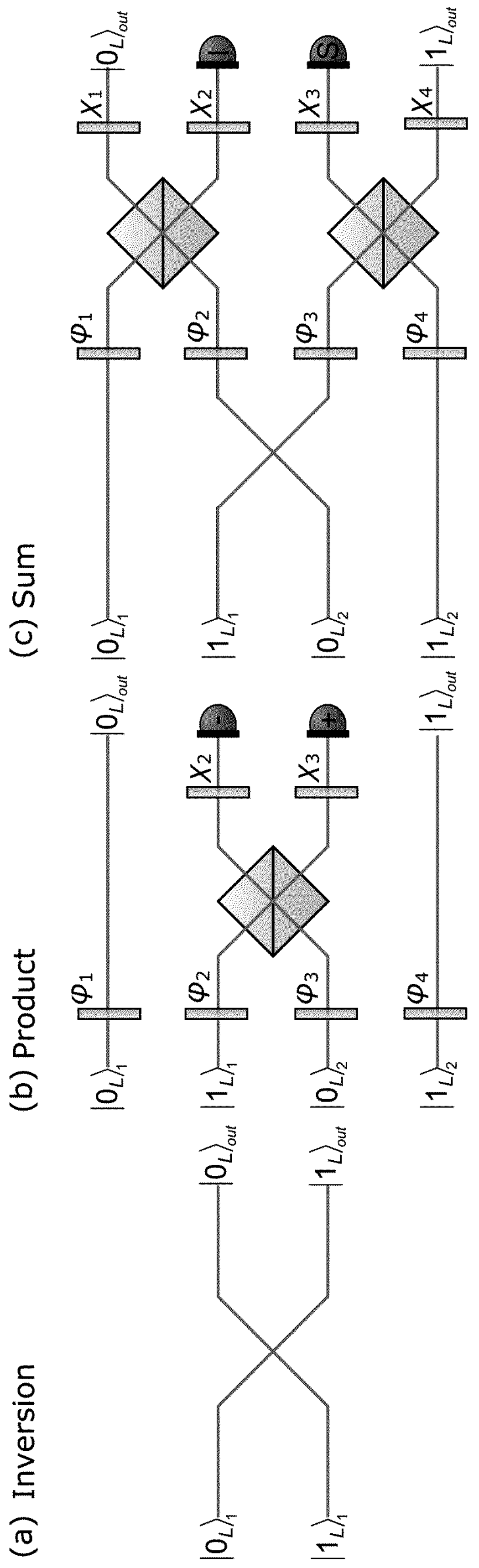

Fig. 5

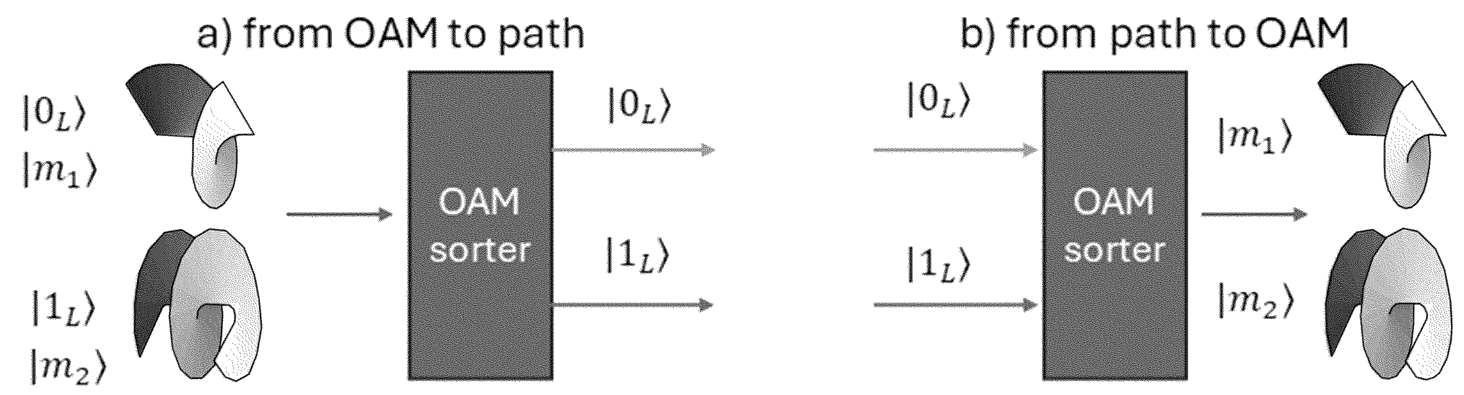
a) from OAM to path
$|0_L\rangle$
$|m_1\rangle$
$|1_L\rangle$
$|m_2\rangle$
OAM sorter
$|0_L\rangle$
$|1_L\rangle$
b) from path to OAM
$|0_L\rangle$
$|1_L\rangle$
OAM sorter
$|m_1\rangle$
$|m_2\rangle$

Fig. 6

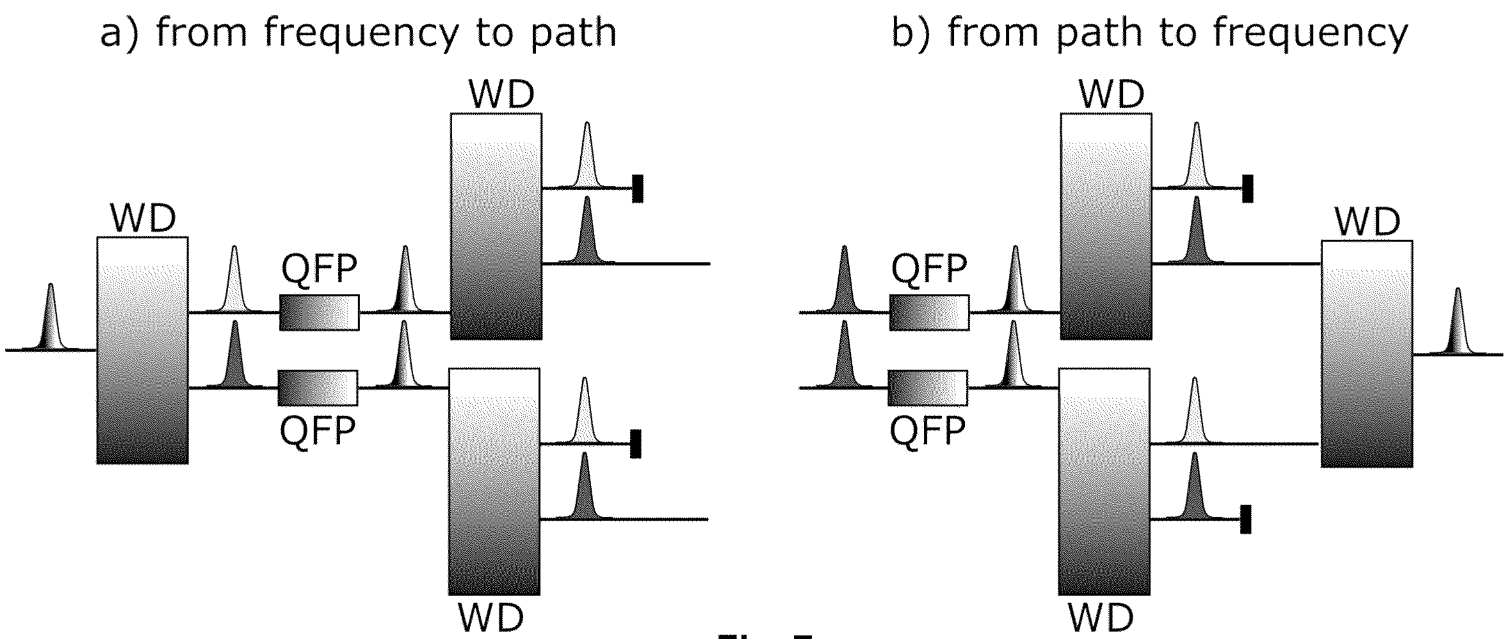
a) from frequency to path
WD
QFP
QFP
WD
WD
b) from path to frequency
QFP
QFP
WD
WD
WD

Fig. 7

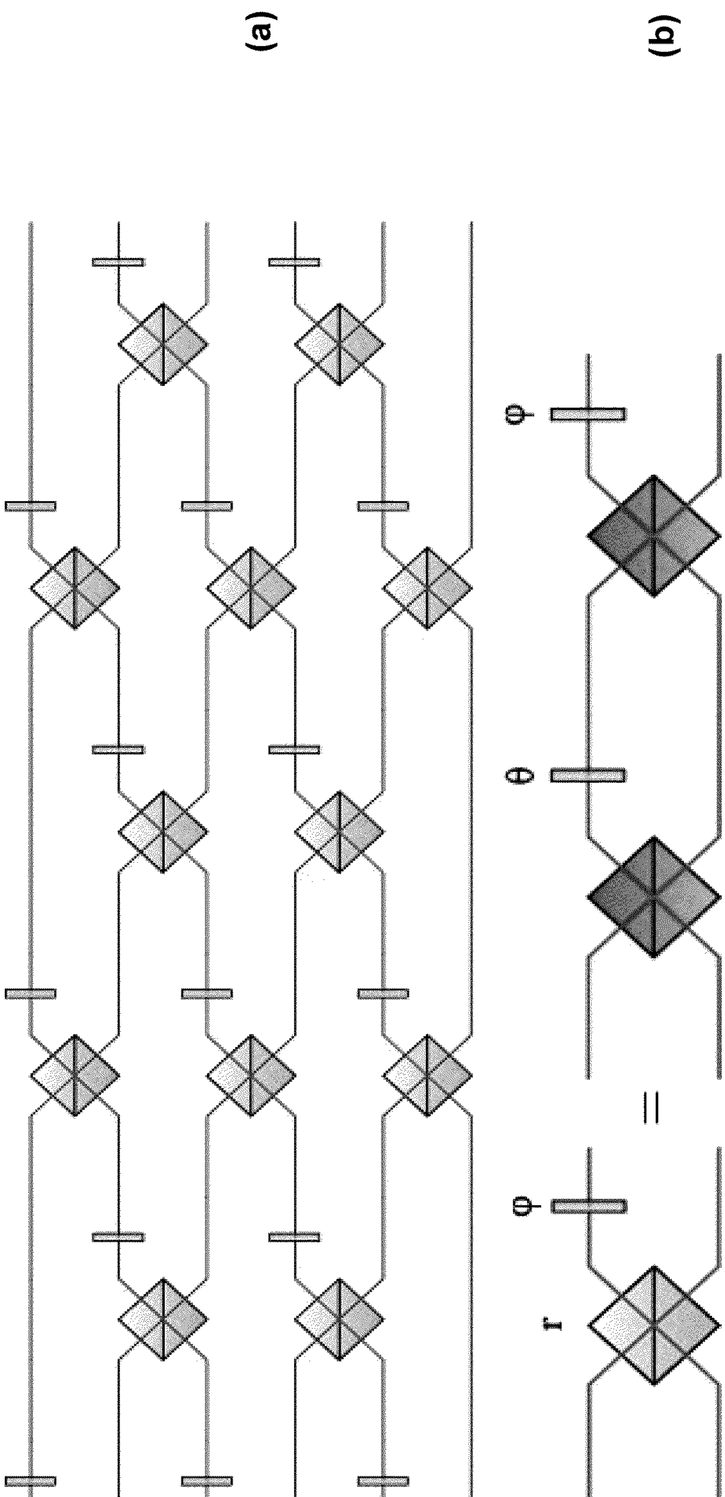

Fig. 8

Fig. 9

(a)

(b)

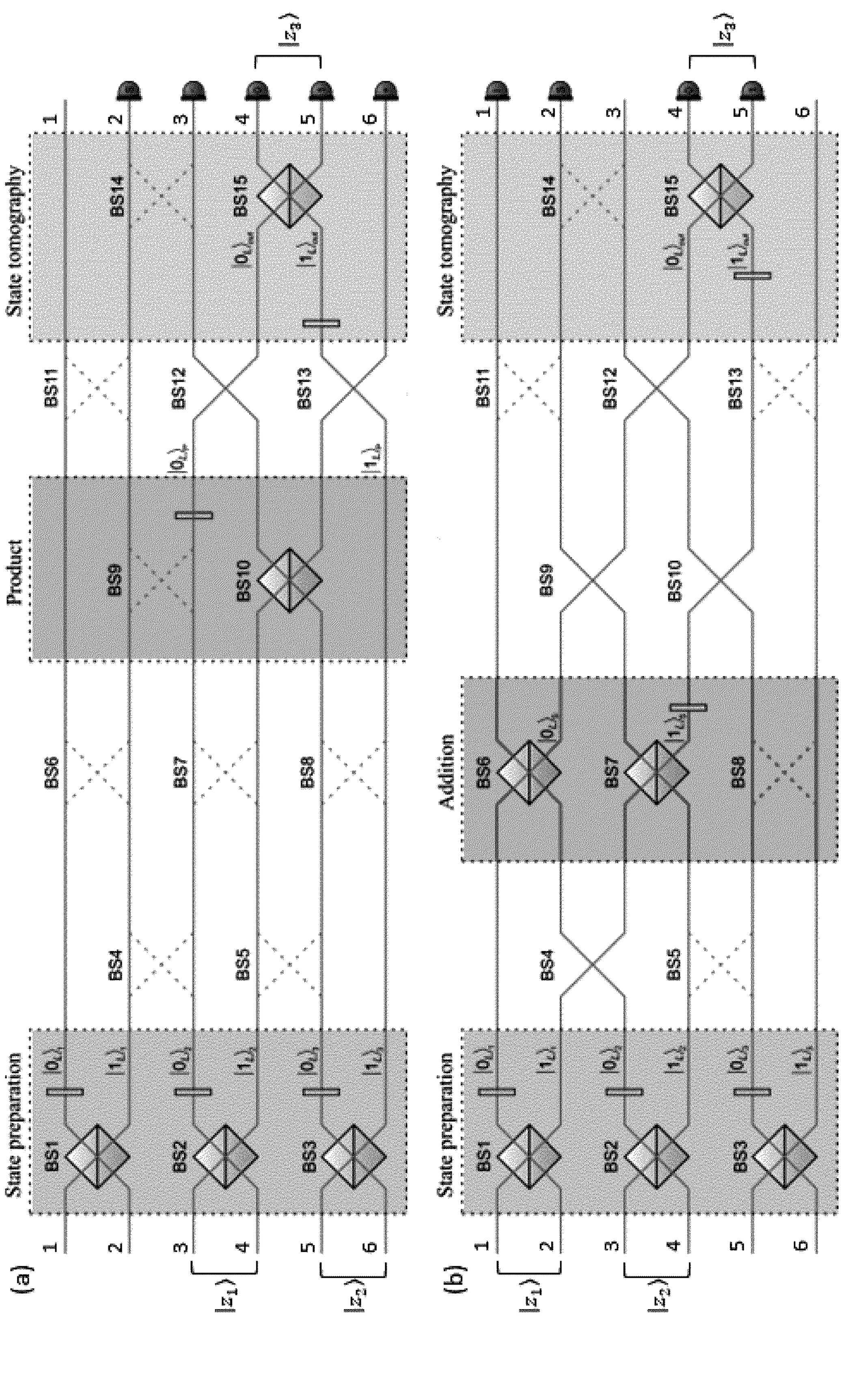
(a)
State preparation
BS1
BS2
BS3
BS4
BS5
BS6
BS7
BS8
Product
BS9
BS10
BS11
BS12
BS13
State tomography
BS14
BS15
$|z_1\rangle$
$|z_2\rangle$
$|z_3\rangle$
(b)
Addition

Fig. 10

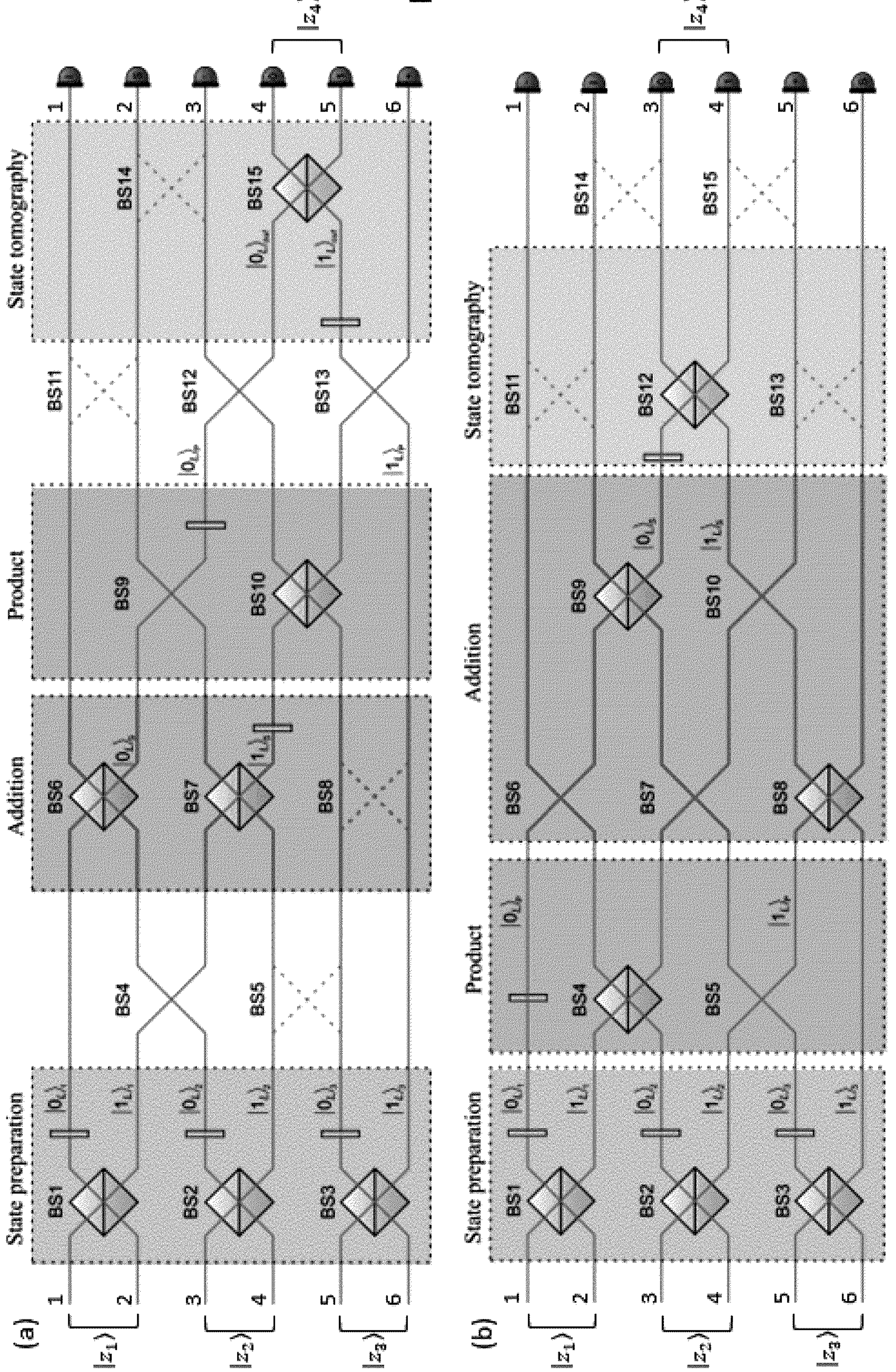
(a)
State preparation
Addition
Product
State tomography
BS1
BS2
BS3
BS4
BS5
BS6
BS7
BS8
BS9
BS10
BS11
BS12
BS13
BS14
BS15
(b)
State preparation
Product
Addition
State tomography

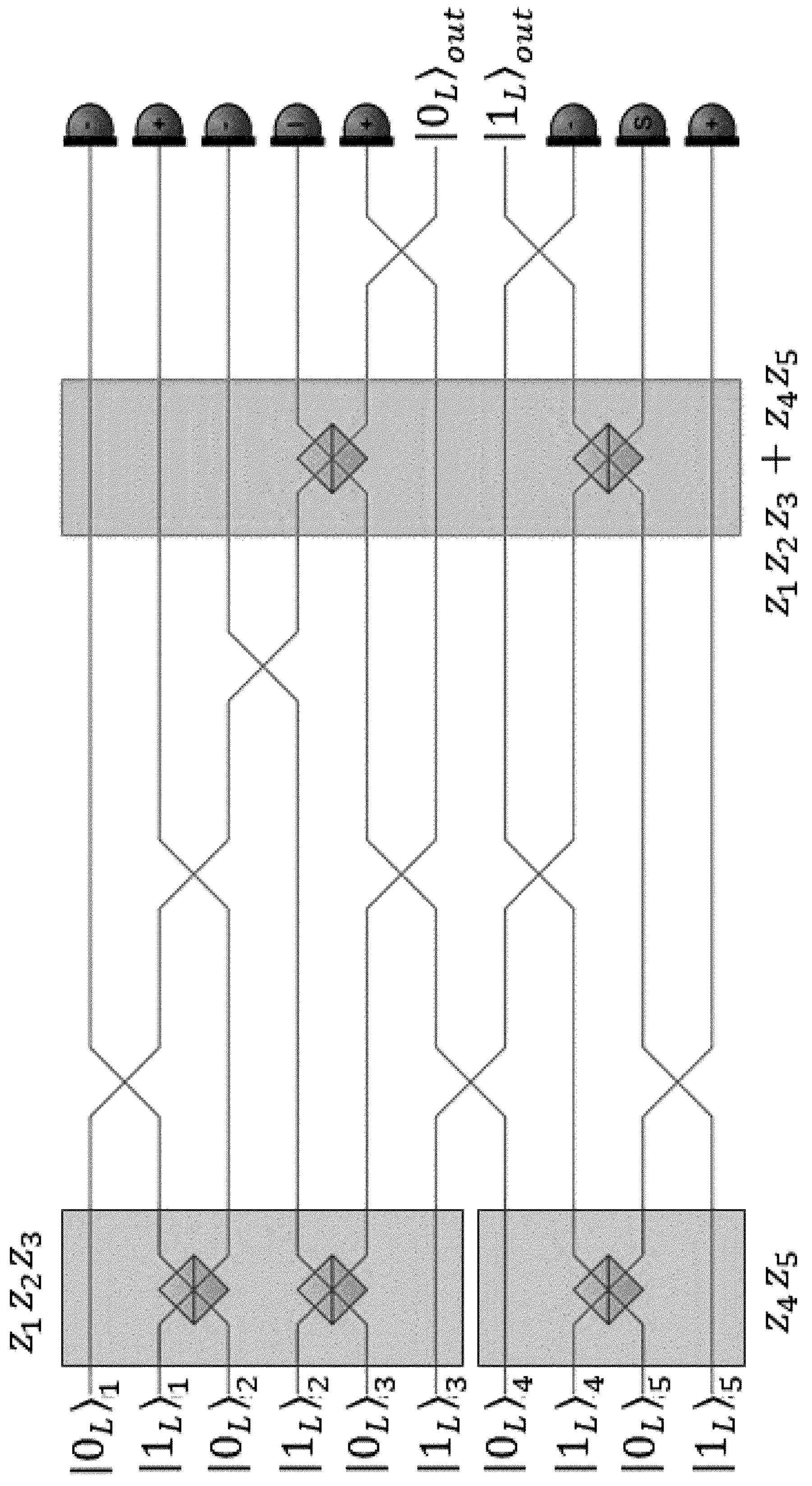
$|0_L\rangle_1$
$|1_L\rangle_1$
$|0_L\rangle_2$
$|1_L\rangle_2$
$|0_L\rangle_3$
$|1_L\rangle_3$
$|0_L\rangle_4$
$|1_L\rangle_4$
$|0_L\rangle_5$
$|1_L\rangle_5$
$Z_1 Z_2 Z_3$
$Z_4 Z_5$
$Z_1 Z_2 Z_3 + Z_4 Z_5$
$|0_L\rangle_{out}$
$|1_L\rangle_{out}$

Fig. 11

INTERNATIONAL SEARCH REPORT

International application No
PCT/EP2024/065333

A. CLASSIFICATION OF SUBJECT MATTER
INV. G06F7/544 G06E3/00 G06N10/00
ADD.

According to International Patent Classification (IPC) or to both national classification and IPC

B. FIELDS SEARCHED

Minimum documentation searched (classification system followed by classification symbols)
G06F G06N G06E

Documentation searched other than minimum documentation to the extent that such documents are included in the fields searched

Electronic data base consulted during the international search (name of data base and, where practicable, search terms used)

EPO-Internal

C. DOCUMENTS CONSIDERED TO BE RELEVANT

Category*	Citation of document, with indication, where appropriate, of the relevant passages	Relevant to claim No.
A	YONG LIU ET AL: "General Quantum Bernoulli Factory: Framework Analysis and Experiments", ARXIV.ORG, CORNELL UNIVERSITY LIBRARY, 201 OLIN LIBRARY CORNELL UNIVERSITY ITHACA, NY 14853, 27 September 2021 (2021-09-27), XP091041786, DOI: 10.1088/2058-9565/AC2061 Sections II, III, IV, supplementary materials section section III; figure 2 ----- -/--	1-22

[x] Further documents are listed in the continuation of Box C.

[ ] See patent family annex.

* Special categories of cited documents :

"A" document defining the general state of the art which is not considered to be of particular relevance

"E" earlier application or patent but published on or after the international filing date

"L" document which may throw doubts on priority claim(s) or which is cited to establish the publication date of another citation or other special reason (as specified)

"O" document referring to an oral disclosure, use, exhibition or other means

"P" document published prior to the international filing date but later than the priority date claimed

"T" later document published after the international filing date or priority date and not in conflict with the application but cited to understand the principle or theory underlying the invention

"X" document of particular relevance;; the claimed invention cannot be considered novel or cannot be considered to involve an inventive step when the document is taken alone

"Y" document of particular relevance;; the claimed invention cannot be considered to involve an inventive step when the document is combined with one or more other such documents, such combination being obvious to a person skilled in the art

"&" document member of the same patent family

Date of the actual completion of the international search	Date of mailing of the international search report
20 August 2024	06/09/2024

Name and mailing address of the ISA/	Authorized officer
European Patent Office, P.B. 5818 Patentlaan 2 NL - 2280 HV Rijswijk Tel. (+31-70) 340-2040, Fax: (+31-70) 340-3016	Tenbieg, Christoph

2

C(Continuation). DOCUMENTS CONSIDERED TO BE RELEVANT

Category*	Citation of document, with indication, where appropriate, of the relevant passages	Relevant to claim No.
A	JIAQING JIANG ET AL: "Quantum-to-Quantum Bernoulli Factory", ARXIV.ORG, CORNELL UNIVERSITY LIBRARY, 201 OLIN LIBRARY CORNELL UNIVERSITY ITHACA, NY 14853, 28 December 2017 (2017-12-28), XP081507530, DOI: 10.1103/PHYSREVA.97.032303 Section III -----	1-22
A	ZHAN XIANG ET AL: "Experimental demonstration of quantum-to-quantum Bernoulli factory", PHYSICAL REVIEW A, 6 July 2020 (2020-07-06), XP093108322, ISSN: 2469-9926, DOI: 10.1103/PhysRevA.102.012605 Retrieved from the Internet: URL:https://journals.aps.org/pra/pdf/10.1103/PhysRevA.102.012605 [retrieved on 2023-12-04] Sections II, III; figure 1 -----	1-22